https://doi.org/10.1093/plcell/koad064 THE PLANT CELL 2023: 35: 2391–2412

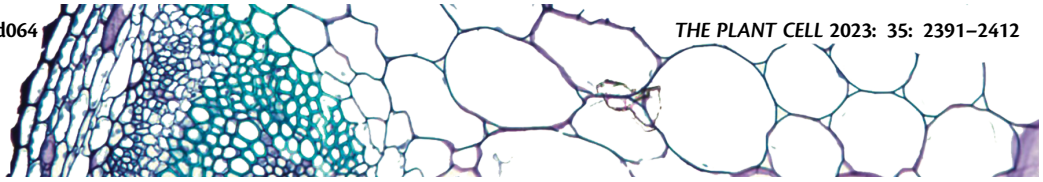

Research Article

# Phosphorylation and ubiquitination of OsWRKY31 are integral to OsMKK10-2-mediated defense responses in rice

**Shuai Wang,† Shuying Han,† Xiangui Zhou,† Changjiang Zhao, Lina Guo, Junqi Zhang, Fei Liu, Qixin Huo, Wensheng Zhao, Zejian Guo and Xujun Chen***

Key Laboratory of Pest Monitoring and Green Management, MOA, Joint Laboratory for International Cooperation in Crop Molecular Breeding, Department of Plant Pathology, China Agricultural University, Beijing 100193, China

*Author for correspondence: chenxj@cau.edu.cn
†These authors contributed equally.
The author(s) responsible for distribution of materials integral to the findings presented in this article in accordance with the policy described in the Instructions for Authors (https://academic.oup.com/plcell/pages/General-Instructions) is: Xujun Chen (chenxj@cau.edu.cn)

## Abstract

Mitogen-activated protein kinase (MPK) cascades play vital roles in plant innate immunity, growth, and development. Here, we report that the rice (*Oryza sativa*) transcription factor gene *OsWRKY31* is a key component in a MPK signaling pathway involved in plant disease resistance in rice. We found that the activation of OsMKK10-2 enhances resistance against the rice blast pathogen *Magnaporthe oryzae* and suppresses growth through an increase in jasmonic acid and salicylic acid accumulation and a decrease of indole-3-acetic acid levels. Knockout of *OsWRKY31* compromises the defense responses mediated by OsMKK10-2. OsMKK10-2 and OsWRKY31 physically interact, and OsWRKY31 is phosphorylated by OsMPK3, OsMPK4, and OsMPK6. Phosphomimetic OsWRKY31 has elevated DNA-binding activity and confers enhanced resistance to *M. oryzae*. In addition, OsWRKY31 stability is regulated by phosphorylation and ubiquitination via RING-finger E3 ubiquitin ligases interacting with WRKY 1 (OsREIW1). Taken together, our findings indicate that modification of OsWRKY31 by phosphorylation and ubiquitination functions in the OsMKK10-2-mediated defense signaling pathway.

## Introduction

Plants have developed sophisticated defense mechanisms during the arms race with pathogens. Preformed defenses include physical barriers and constitutive chemicals with antimicrobial activities. Inducible defenses are triggered during plant–pathogen interactions and include pathogen-associated molecular pattern (PAMP)-triggered immunity (PTI) and effector-triggered immunity (ETI), which are activated to restrict pathogen infection (Jones and Dangl 2006). In general, both PTI and ETI induce similar signal transduction and defense responses, although the ETI response is more pronounced. However, the exact signal transduction that leads to global transcriptional reprogramming remains largely unknown.

PAMPs, such as bacterial flagellin or peptidoglycan and fungal chitin, are perceived by pattern-recognition receptors, activating a signaling cascade. Upon perception of a chitin elicitor, rice (*Oryza sativa*) chitin elicitor-binding proteins dimerize and then form a receptor complex with CHITIN ELICITOR RECEPTOR KINASE 1 (OsCERK1) to initiate the signaling process (Hayafune et al. 2014). OsCERK1 directly phosphorylates RECEPTOR-LIKE CYTOPLASMIC KINASE 185 (OsRLCK185) in response to chitin and is required to activate

Received October 05, 2022. Accepted February 13, 2023. Advance access publication March 3, 2023
© The Author(s) 2023. Published by Oxford University Press on behalf of American Society of Plant Biologists.
This is an Open Access article distributed under the terms of the Creative Commons Attribution-NonCommercial-NoDerivs licence (https://creativecommons.org/licenses/by-nc-nd/4.0/), which permits non-commercial reproduction and distribution of the work, in any medium, provided the original work is not altered or transformed in any way, and that the work is properly cited. For commercial re-use, please contact journals.permissions@oup.com

Open Access

a mitogen-activated protein kinase (MPK) cascade (Yamaguchi et al. 2013). MPKs are important players in many biological processes, including responses to abiotic and biotic stresses in plants. In each MPK cascade, a MPK is phosphorylated by a MPK kinase (MKK), which may be activated by an MKK kinase (MKKK). The activated MPK can phosphorylate target proteins to confer their responses to environmental cues and developmental requirements. The rice genome contains 74 MKKKs, eight MKKs, and 17 MPKs (Hamel et al. 2006; Reyna and Yang 2006; Yang et al. 2015); MKKs are particularly important because they are considered the convergence points in the MPK signaling modules (Andreasson and Ellis 2010).

In rice, OsMPK3 interacts with SUBMERGENCE1A1 (SUB1A1), an ethylene response factor-like protein, regulating submergence tolerance in rice (Singh and Sinha 2016). Activation of OsMPK4 can enhance rice resistance against *Xanthomonas oryzae* pv. *oryzae* (*Xoo*), the causal pathogen of bacterial blight disease (Shen et al. 2010). Chitin induces the OsMKK4–OsMPK3/OsMPK6 cascade for cell death and biosynthesis of diterpenoid phytoalexins and lignin (Kishi-Kaboshi et al. 2010). OsMKK4 can be phosphorylated by OsMKKK18 and OsMKKKϵ, and in turn, OsMKKKϵ is phosphorylated by OsRLCK185 (Wang et al. 2017; Yamada et al. 2017). Interestingly, the OsMKKK10–OsMKK4–OsMPK6 signaling pathway positively controls grain size and weight (Guo et al. 2018; Xu et al. 2018). Moreover, OsMKK10-2 has been reported to activate OsMPK3 and OsMPK6 for enhanced resistance to a bacterial streak pathogen, *X. oryzae* pv. *oryzicola* (*Xoc*), and tolerance to drought stress (Ma et al. 2017). OsMKK10-2–OsMPK6 pathway is required for OsWRKY45-mediated resistance against *Magnaporthe oryzae* (Ueno et al. 2013). Recently, OsMPK6 has been shown to phosphorylate a Raf-like kinase ENHANCED DISEASE RESISTANCE 1 (OsEDR1), leading to increased OsMKK10-2 activity and resistance to *Xoc* (Ma et al. 2021).

Auxins regulate many processes of growth and development in plants, including petiole elongation, root architecture, and gravity perception (Kazan 2013), and implicated in promoting disease susceptibility in *Arabidopsis thaliana* (Chen et al. 2007; Kidd et al. 2011). In this context, flg22 induces accumulation of *Arabidopsis* microRNA393 (miR393), which targets the auxin F-box receptor genes *TRANSPORT INHIBITOR 1* (*TIR1*), *AUXIN SIGNALING F-BOX 2* (*AFB2*), and *AFB3*, resulting in repression of auxin signaling and restriction of *Pseudomonas syringae* growth (Navarro et al. 2006). Overexpression of NONEXPRESSOR OF PATHOGENESIS-RELATED 1 (*OsNPR1*) increases resistance to *Xoo* but attenuates rice growth (Yuan et al. 2007). A later study suggested that the indole-3-acetic acid (IAA) content and the auxin distribution pattern are altered in *OsNPR1*-overexpressing plants, partially owing to the upregulation of IAA–amido synthase gene *GRETCHEN HAGEN 3.8* (*OsGH3.8*) (Li et al. 2016). Constitutive expression of *OsGH3.8* in rice reduces free IAA content, suppresses plant growth, and enhances resistance to bacterial pathogen *Xoo* (Ding et al. 2008). In *Arabidopsis*, the activation-tagged *bushy and dwarf 1* (*bud1*) mutant, which results from the increased expression of the *MKK7* gene, inhibits auxin transport indicating that MKK7 negatively regulates polar auxin transport (PAT) (Dai et al. 2006). Conversely, *bud1* mutant accumulates elevated amounts of salicylic acid (SA) and displays enhanced resistance to pathogens. In this context, MKK7 phosphorylates MPK3 and MPK6 *in planta* and positively modulates plant basal and systemic acquired resistance (Zhang et al. 2007; Jia et al. 2016).

WRKY transcription factors (TFs) participate in various plant processes, including growth, development, and responses to abiotic and biotic stresses (Chen et al. 2019). In previous studies, we showed that OsWRKY31 (renamed as OsWRKY55, Rice WRKY Working Group 2012) and OsWRKY89 are positive regulators of rice resistance against *M. oryzae* (Wang et al. 2007; Zhang et al. 2008). Both OsWRKY31 and OsWRKY89 belong to the WRKY IIIb subclade, which formed after the divergence of *Arabidopsis* and rice (Wu et al. 2005). In a yeast two-hybrid (Y2H) screen using OsWRKY89 as a bait, OsMKK10-2 and OsREIW1 were obtained as interactors, and these proteins also interact with OsWRKY31. Here, we revealed that OsWRKY31 acts as a key regulator downstream of OsMKK10-2 and OsMPK3 is also a downstream component of the kinase. Moreover, OsWRKY31 stability was affected by its phosphorylation and ubiquitination statuses. Our study sheds light on post-transcriptional regulation of plant immunity.

## Results

### OsWRKY31 physically interacts with OsMKK10-2 and OsMPKs

The interaction between OsMKK10-2 and OsWRKY31 was tested in yeast cells with OsMKK10-2 and OsWRKY31 fused with the Gal4 DNA-binding domain (in pBD bait vector) and activation domain (in pAD prey vector), respectively. The interaction between OsMKK10-2 and OsWRKY31 was confirmed by the growth of yeast cells harboring BD-OsMKK10-2 and AD-OsWRKY31 plasmids on the selection media deficient in Leu, Trp, His, and adenine (-LWHA; Fig. 1A). However, no interaction was observed between OsMKK10-2 and OsWRKY76.1 or OsWRKY45, suggesting a specific interaction between OsMKK10-2 and OsWRKY31. For protein pull-down assays, OsMKK10-2 and OsWRKY31 were expressed as GST-MKK10-2-3myc with glutathione transferase (GST) and 3×Myc epitope tags and GST-WRKY31-3flag, respectively, in *Escherichia coli*; GST-WRKY31-3flag was found to interact specifically with GST-MKK10-2-3myc (Fig. 1B).

To validate the interaction between OsWRKY31 and OsMKK10-2 *in planta*, OsMKK10-2 and OsWRKY31 were fused with N- or C-terminal parts of a split yellow fluorescent protein (YFP) for bimolecular fluorescence complementation

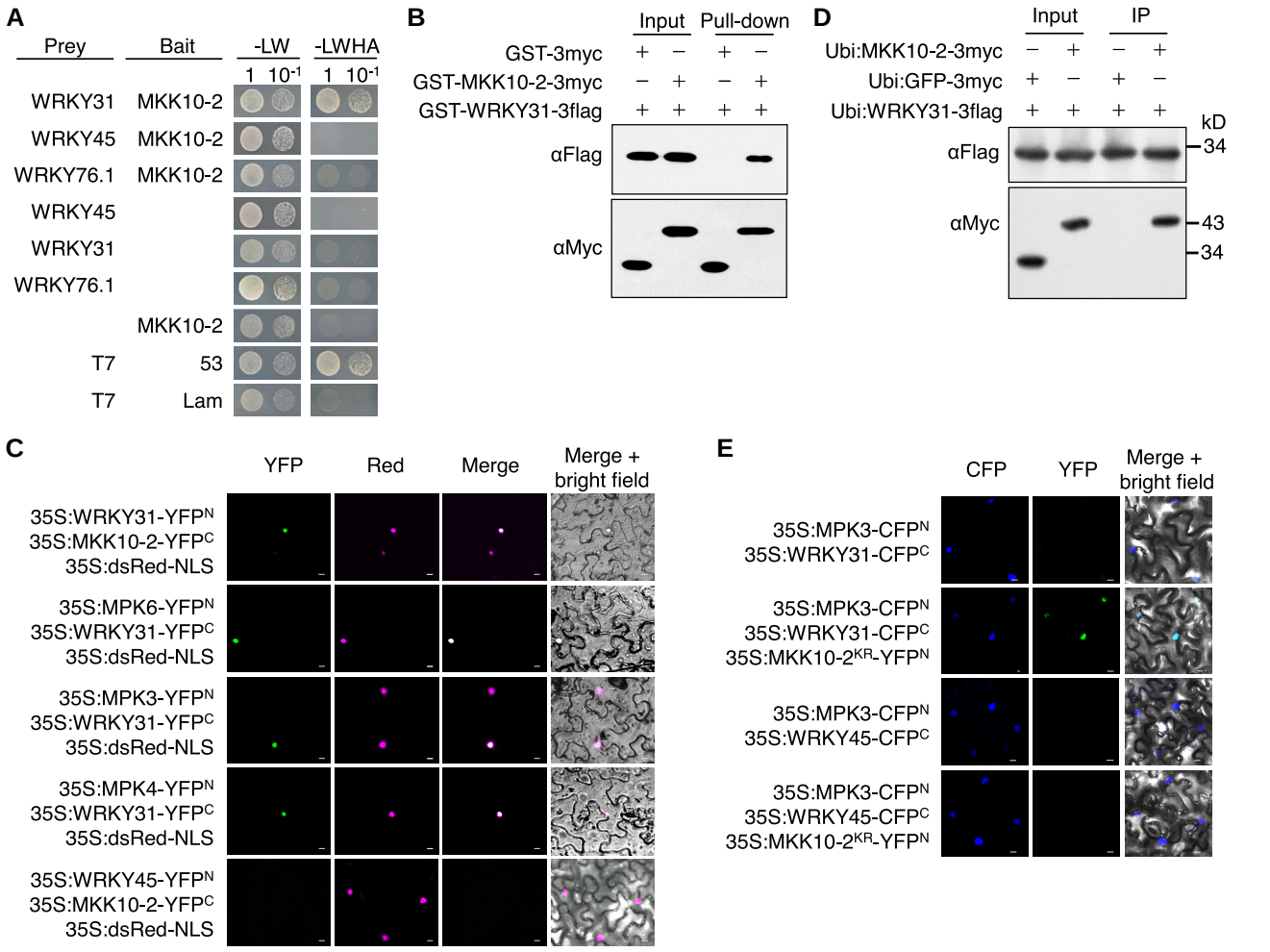


**Figure 1.** OsMKK10-2 and OsMPKs interact with OsWRKY31. **A)** OsWRKY31, OsWRKY45, OsWRKY76.1, and OsMKK10-2 were fused to the Gal4 activation domain (prey) or DNA-binding domain (bait). The resulted plasmids in appropriate combinations were introduced into yeast cells and then incubated in synthetic dropout medium without Leu and Trp (-LW) or lacking Leu, Trp, His, and adenine (-LWHA) and photographed 3 d after plating. Yeast cells containing AD-T7 plus BD-53, and AD-T7 plus BD-Lam plasmids were used as the positive and negative controls, respectively. **B)** OsMKK10-2 and OsWRKY31 were sandwiched with GST and 3×Myc (GST-MKK10-2-3myc) or GST and 3×Flag (GST-WRKY31-3flag) tags. Purified protein (each about 1 μg) was combined accordingly and incubated at 4 °C for 2 h in immunoprecipitation buffer. The protein mixture was precipitated with anti-c-Myc agarose affinity gels, separated on 10% SDS-PAGE gels, and detected by immunoblots with αMyc and αFlag antibodies. **C)** OsWRKY31, OsWRKY45, OsMKK10-2, OsMPK3, OsMPK4, and OsMPK6 were fused in frame with the YFP N-terminal region ($YFP^N$) or the YFP C-terminal region ($YFP^C$). The *Agrobacteria* with combined plasmids were infiltrated into the leaves of *N. benthamiana*. Confocal images were taken at 2 d after the infiltrations. Red fluorescence signals indicative of the nuclei were from co-infiltrated 35S:dsRed-NLS (NLS: nuclear localization signal). **D)** Plasmids of Ubi:MKK10-2-3myc, Ubi:WRKY31-3flag, and Ubi:GFP-3flag control were introduced separately in *A. tumefaciens* and co-expressed in appropriate combinations in leaves of *N. benthamiana*. Total proteins were extracted and immunoprecipitated with anti-c-Flag affinity gels. The precipitates were subjected for immunoblots with αMyc and αFlag antibodies. **E)** OsWRKY31 or OsWRKY45 and OsMPK3 were fused with $CFP^C$ and $CFP^N$, respectively. $OsMKK10\text{-}2^{KR}$, a kinase-dead mutant with $Lys^{81}$ to $Arg^{81}$ substitution, was fused with $YFP^N$. Images photographed at 2 d after the infiltrations are CFP (left), YFP (middle), and merged with bright field (right). Bar = 10 μm.

(BiFC) assays. The 35S:MKK10-2-$YFP^C$ and 35S:WRKY31-$YFP^N$ plasmids were co-expressed with nuclear localization signal-targeted dsRED (35S:dsRED-NLS) in *Nicotiana benthamiana* leaves via *Agrobacterium tumefaciens*-mediated infiltration. The detection of YFP fluorescence indicated the interaction of MKK10-2-$YFP^C$ with WRKY31-$YFP^N$; the co-localization of YFP and RED fluorescence signals indicated that the interaction occurred exclusively in the nuclei of *N. benthamiana* epidermal cells (Fig. 1C). OsWRKY45, belonging to the WRKY IIIa subclade, functions in the OsMKK10-2–OsMPK6 cascade (Ueno et al. 2015). Interaction between WRKY45-$YFP^N$ and MKK10-2-$YFP^C$ was not detected. The interaction of OsMKK10-2 with OsWRKY31 was also confirmed by the transient expression of Ubi:MKK10-2-3myc and Ubi:WRKY31-3flag proteins in *N. benthamiana* leaves using co-immunoprecipitation (CoIP) (Fig. 1D).

OsMKK10-2 has been found to interact with OsMPK3, OsMPK4, and OsMPK6 but not with OsMPK17-1 (Zhou et al. 2017). Thus, we further tested the interactions between OsWRKY31 with these OsMPKs and found that OsMPK3, OsMPK4, and OsMPK6 were able to interact with OsWRKY31 in yeast cells (Supplemental Fig. S1). Physical interactions of OsWRKY31 with the three OsMPKs were further revealed by BiFC assays using 35S:WRKY31-YFP$^N$ co-transformed with 35S:MPK3-YFP$^N$, 35S:MPK4-YFP$^N$, or 35S:MPK6-YFP$^N$ in epidermal cells of *N. benthamiana* leaves with a dsRed-fused nuclear marker. The co-localization of YFP and red fluorescence signals indicated that the interactions occurred in the nuclear compartment (Fig. 1C).

Furthermore, multicolor BiFC analysis was used to test the complex formation among OsWRKY31, OsMPK3, and OsMKK10-2$^{KR}$ (the kinase-dead mutant generated by changing the amino acid Lys$^{81}$ to Arg), as OsMKK10-2 caused cell death in *N. benthamiana* leaves, especially in the presence of OsMPKs (Kamigaki et al. 2016; Zhou et al. 2017). Two types of fluorescence signals were visualized among WRKY31-CFP$^C$, MPK3-CFP$^N$, and MKK10-2$^{KR}$-YFP$^N$ in the *N. benthamiana* cells but not with WRKY45-CFP$^C$ substitution of WRKY31-CFP$^C$ (Fig. 1E), revealing the formation of OsWRKY31–OsMPK3–OsMKK10-2$^{KR}$ nuclear complex. These results indicate that OsWRKY31 can physically interact with OsMPK3 and its upstream OsMKK10-2, forming a ternary complex.

## OsWRKY31 is phosphorylated by the OsMKK10-2–OsMPK module

To examine whether OsMKK10-2 could activate the phosphorylation of OsMPKs and OsWRKY31, we first analyzed the autophosphorylation activity of OsMKK10-2. The amino acids Arg$^{203}$ and Ser$^{209}$ of OsMKK10-2 were mutated into Asp (OsMKK10-2$^{DD}$) for constitutive activation, although OsMKK10-2 did not contain the typical S/T-X$_5$-S/T motif for a MKKK phosphorylation (Hamel et al. 2006). Autophosphorylation activities were observed for the recombinant GST-MKK10-2$^{DD}$-3myc protein and, to a lesser extent, for the wild-type GST-MKK10-2-3myc, but not for the kinase-dead mutant GST-MKK10-2$^{KR}$-3myc (Supplemental Fig. S2A).

Second, we investigated the phosphorylation of OsWRKY31 by OsMPK proteins in vitro using Phos-tag gel assays. The migration of phosphorylated GST-WRKY31-3flag proteins was clearly retarded for samples treated with GST-MPK3-3myc and GST-MPK4-3myc, while no significant retarded bands were found for those treated with only GST-MPK6-3myc, GST-MKK10-2-3myc, or GST-MKK10-2$^{DD}$-3myc. However, GST-WRKY31-3flag was markedly phosphorylated when GST-MPK6-3myc was added in combination with GST-MKK10-2-3myc or GST-MKK10-2$^{DD}$-3myc (Fig. 2A), suggesting that the activation of OsMPK6 via OsMKK10-2 was required for OsWRKY31 phosphorylation in vitro.

Third, we examined whether OsMKK10-2 activated phosphorylation of OsMPKs and OsWRKY31 *in planta*. Dexamethasone (Dex)-inducible MKK10-2-myc plants and knockout plants of *OsMKK10-2* (*mkk10-2ko*), *OsMPK3* (*mpk3ko*), and *OsWRKY31* (*w31ko*) were obtained through the CRISPR/Cas9 method (Supplemental Fig. S3). Rice seedlings harboring the Dex:MKK10-2-myc construct were treated with Dex or dimethyl sulfoxide (DMSO) solvent as control, and sampled for immuno-blot analysis. The prominent phosphorylation of OsMPK6 and OsMPK3 was detected after Dex treatment using anti-pTEpY antibody, while in Dex:MKK10-2 *mpk3ko* plants, the DEX treatment failed to activate OsMPK3 phosphorylation (Fig. 2B, Supplemental Fig. S2B), suggesting that OsMPK3 was also a component downstream of OsMKK10-2 phosporylation cascade. Moreover, using an antibody for detection of specific phosphorylation of OsWRKY31 at Ser$^6$ (anti-W31pS6) (Supplemental Fig. S4), an increase of OsWRKY31 phosphorylation levels was observed in Dex-induced plants compared with the mock treatment (Fig. 2B). Furthermore, chitin-induced OsWRKY31 accumulation was reduced in the *mpk3ko* background, although the relative amounts of phosphorylated OsWRKY31 vs. total OsWRKY31 were found to be somewhat variable in different experiments (Fig. 2C).

## OsWRKY31 is a key player in OsMKK10-2-mediated resistance against *M. oryzae*

To examine whether *OsWRKY31* acts downstream of *OsMKK10-2* during defense responses, the transgenic and wild-type plants were inoculated with the rice blast fungus *M. oryzae*. Spores of *M. oryzae* SZ strain were injected into the leaf sheaths of rice plants (about 3-mo-old), and the newly grown leaves were collected for disease evaluation. The *mkk10-2ko* and *w31ko* plants were more susceptible to *M. oryzae* SZ than those of Zhonghua 17 (ZH17), whereas the *OsWRKY31*-overexpressing plants showed reduced susceptibility to the SZ strain compared with the ZH17 controls (Supplemental Fig. S5). However, introduction of Ubi:fW31h into the *mkk10-2ko* and *mpk3ko* background significantly decreased the susceptibility to *M. oryzae* (Fig. 3, A and B). To activate OsMKK10-2, Dex:MKK10-2-myc and Dex:MKK10-2 *w31ko* plants were sprayed with Dex 12 h before the pathogen inoculation. Dex-induced expression of *OsMKK10-2* enhanced plant resistance to *M. oryzae*, but the resistance was eliminated when the *OsWRKY31* gene was disrupted in the Dex:MKK10-2 *w31ko* lines (Fig. 3, C and D). Conversely, knocking out *OsMPK3* only partially attenuated *OsMKK10-2*-conferred resistance against rice blast fungus. Taken together, these data strongly indicate that OsWRKY31 is a key player in OsMKK10-2-mediated resistance against *M. oryzae* at a wide period of vegetative stage.

## OsMKK10-2 alters auxin distribution and accumulation

Phylogenetic analysis revealed that OsMKK10-2 is a homolog of *Arabidopsis* MKK10, belonging to the same D group as MKK7 (Supplemental Fig. S6) (Hamel et al. 2006). The

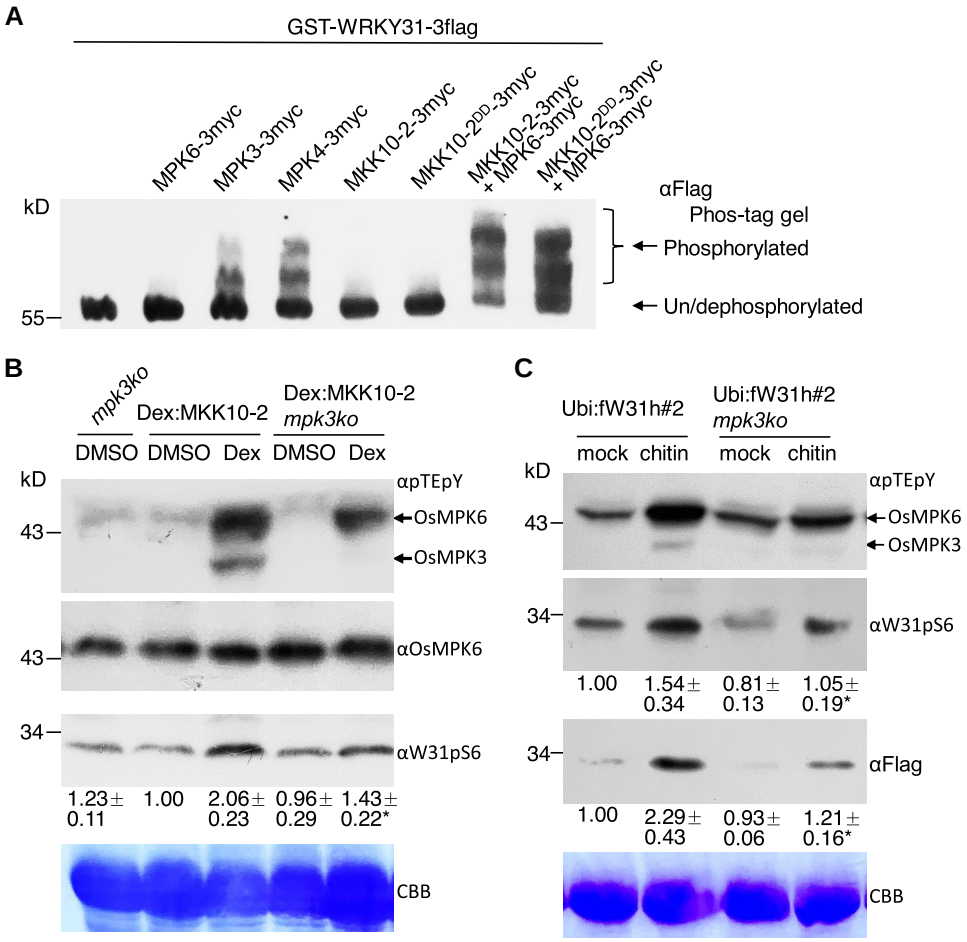


**Figure 2.** OsMKK10-2 activates phosphorylation of OsMPKs and OsWRKY31. **A)** The recombinant proteins were expressed with GST plus 3×Myc or 3×Flag tag. GST-WRKY31-3flag with appropriate combination of kinase(s) were subjected to phosphorylation at 30 °C for 2 h. Proteins were separated on Phos-tag gels and blotted with αFlag antibody. The retarded bands indicated the phosphorylated GST-WRKY31-3flag. OsMKK10-$2^{DD}$: mutations of $Arg^{203}$ and $Ser^{209}$ to Asp for constitutive activation. **B)** Seven-day-old seedlings cultured hydroponically were treated with 10 μM dexamethasone (Dex) or DMSO as the mock. Proteins extracted were separated on 10% SDS-PAGE gels and blotted with αpTEpY, αOsMPK6, or αW31pS6 (generated for detection of OsWRKY31 S6 phosphorylation) antibody. Representative data from four independent experiments. **C)** Ubi:fW31h#2 *mpk3ko* and Ubi:fW31h#2 seedlings were grown hydroponically for 7 d, and then treated with 200 μg $mL^{-1}$ chitin. The proteins extracted were analyzed by immunoblots with αpTEpY, αW31pS6, and αFlag. CBB, Coomassie brilliant blue staining for loading control. Representative data from three independent experiments. Relative intensity (numbers below the gels) of bands was analyzed using ImageJ software. The values below indicate the relative gray density of three experiments. The value marked with * indicates statistically significant difference between Dex treatment **B)** and chitin **C)**, analyzed by the Student's *t*-test (*, $P < 0.05$). Dex:MKK10-2 for Dex:MKK10-2-myc; *mpk3ko* for *OsMPK3* knockout; Ubi:fW31h for Ubi:Flag-WRKY31-6×His.

gain-of-function *bud1* mutant with increased *MKK7* expression exhibits PAT deficiency (Dai et al. 2006). To know whether OsMKK10-2 is involved in auxin transportation, we measured basipetal movement of tritium-labeled IAA ($^3$H-IAA) in the etiolated hypocotyls of the transgenic plants overexpressing OsMKK10-2. The $^3$H-IAA transport in hypocotyl segments of Dex:MKK10-2-myc plants was reduced to ∼60% of that in the control plants 12 h after Dex treatment, whereas the levels of auxin transport were similar between Dex:MKK10-2 *w31ko* and ZH17-control plants (Fig. 4A). The basipetal PAT was significantly inhibited in *OsWRKY31*-overexpressing hypocotyls and enhanced in *mkk10-2ko* segments when compared with the control plants (Fig. 4A).

To further illustrate the impact of OsMKK10-2 on auxin levels, an auxin responsive reporter line was crossed with the Dex:MKK10-2-myc plant to generate the DR5:GUS Dex:MKK10-2 progeny. To visualize the distribution of auxin in vivo, GUS staining was performed from the early stage of seed germination on the resulting seedlings treated with Dex or DMSO solvent. A marked reduction of GUS staining was observed on germinating seeds 24 h after Dex treatment (Fig. 4Ba, b), suggesting the decrease of free auxin levels during seed germination when OsMKK10-2 protein was induced. In the 5-d-old seedlings, the Dex treatment also reduced the GUS activity in the leaves and upper part of the primary roots but enhanced the staining in the lower part of the primary

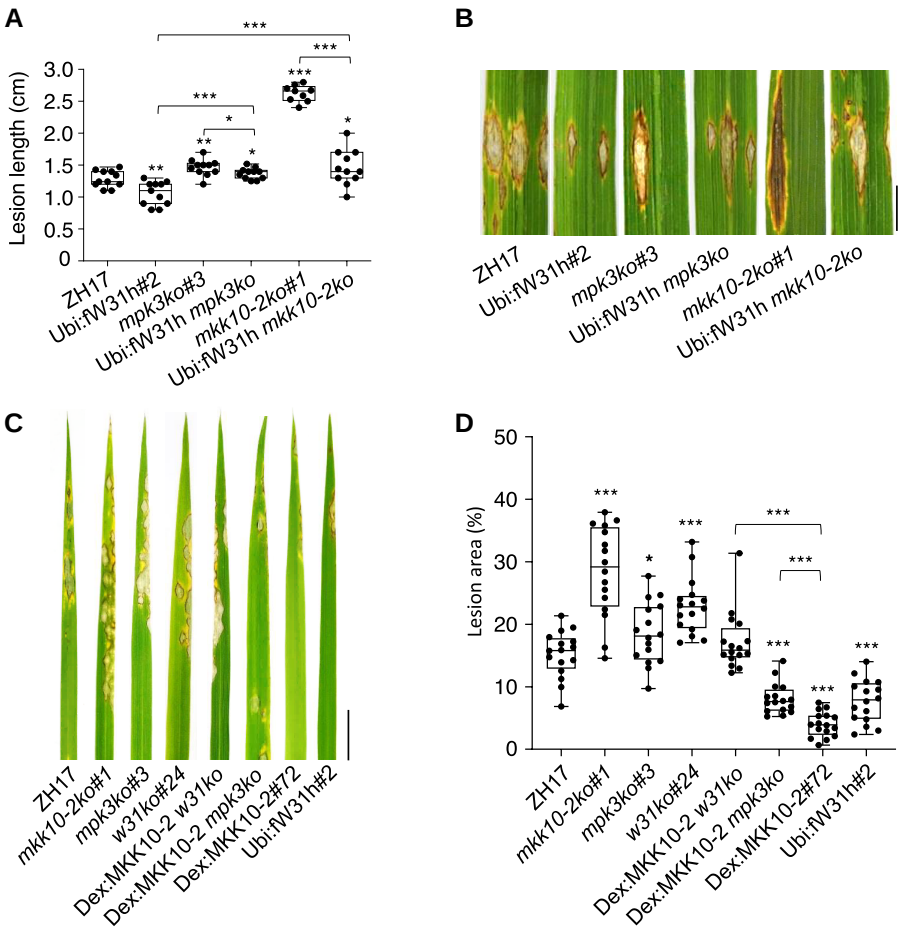


**Figure 3.** *OsWRKY31* and *OsMPK3* are involved in *OsMKK10-2* activated disease resistance. Lesion length **A)** and disease symptoms **B)** of the transgenic and wild-type ZH17 plants after infiltration with *M. oryzae* SZ strain. Plants of tillering stage (about 3-mo-old) in paddy field were injected with SZ spores ($1 \times 10^5$ conidia $mL^{-1}$) in year 2020. The segments of leaves were photographed and quantified at 9 d after the infiltrations. The median was the crossline in each boxplot showing the lesion length distributions ($n \geq 9$). Disease symptoms **C)** and lesion areas **D)** of the transgenic and ZH17 plants infected with SZ strain by spraying. Eighteen-day-old plants were inoculated with SZ spores ($5 \times 10^5$ conidia $mL^{-1}$) by foliar spraying; the Dex-inducible lines were treated with 20 μM Dex for 12 h before the pathogen inoculation and the other plants were received with DMSO as the mock. Evaluation of disease severity and photography taken were conducted at 7 d after the inoculation. Ubi:fW31h *mkk10-2ko* for Ubi:fW31h and *mkk10-2ko* genetic crossing progeny; other plants described in Fig. 2. The median was the crossline in each boxplot showing the lesion area distributions ($n = 16$). Significance was evaluated by comparing with ZH17 or each other as bracketed using the Student's *t*-test (*, $P < 0.05$; **, $P < 0.01$; ***, $P < 0.001$). Bar = 1 cm.

roots (Fig. 4, Bc and C). These observations suggested a potential perturbation of auxin distribution in plant tissues upon activation of OsMKK10-2 expression.

We then investigated the expression of genes related to auxin metabolism and signaling in Dex:MKK10-2-myc plants. *OsGH3.1* and *OsGH3.8* genes, encoding members of the GH3 family of IAA–amido synthetases, are implicated in auxin homeostasis by conjugating free IAA (Ding et al. 2008; Domingo et al. 2009; Li et al. 2016). Levels of *OsGH3.1* and *OsGH3.8* expression were remarkably increased by the activation of *OsMKK10-2* transcription (Fig. 4D). Other genes of the *OsGH3* family such as *OsGH3.2*, *OsGH3.6*, and *OsGH3.9* were upregulated, whereas *OsGH3.4* was downregulated in Dex-treated Dex:MKK10-2-myc plants at the time point examined (Supplemental Fig. S7). The *YUCCA* (*YUC*) family of flavin monooxygenase genes encodes the rate-limiting enzymes in IAA biosynthesis via the tryptophan-dependent pathway (Yamamoto et al. 2007). OsARF12 and OsARF16 are transcriptional activators in regulating auxin response genes and affect auxin transport and root elongation (Qi et al. 2012; Shen et al. 2015). The levels of *OsYUCCA1*, *OsARF12*, and *OsARF16* expression were decreased in Dex-induced Dex:MKK10-2-myc plants (Fig. 4D). Collectively, the results indicate that OsMKK10-2 regulates auxin homeostasis and signaling.

To examine possible growth phenotypes of *OsMKK10-2* expression, the germinated Dex:MKK10-2-myc seeds were transferred onto half strength Murashige and Skoog (MS) medium containing different concentrations of Dex. Root and coleoptile growth of Dex:MKK10-2-myc seedlings was

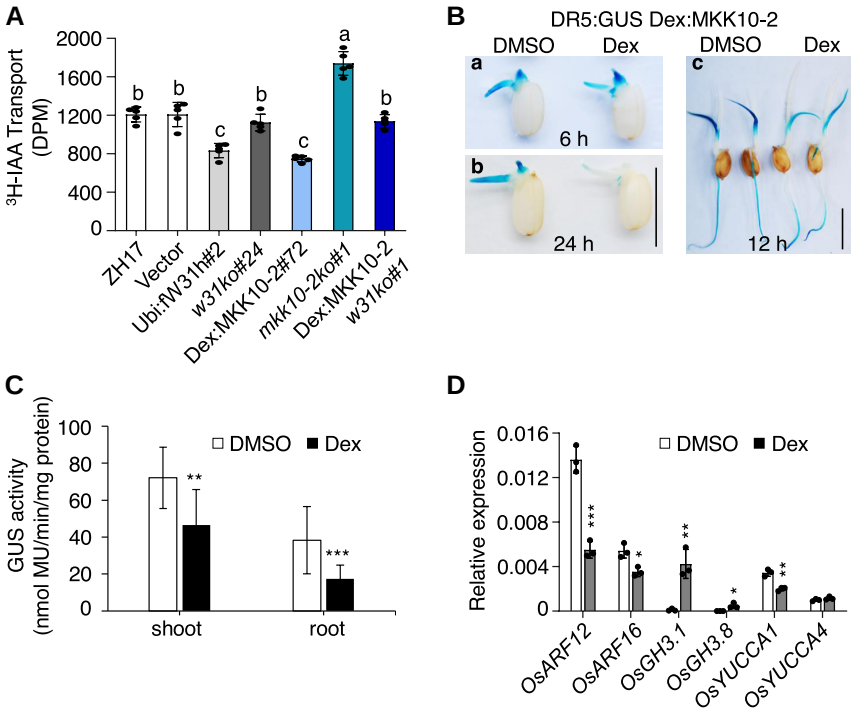


**Figure 4.** Activation OsMKK10-2 suppresses auxin transport and homeostasis. **A)** Polar auxin transport (PAT) assay of coleoptiles. Seven-day-old seedlings growing in the dark were treated with 10 μM Dex for 12 h and then segmented for PAT assay. Values shown are means ± SD of five independent replicates. Values marked with different letters indicate statistically significant differences as analyzed by Duncan's multiple range test, $\alpha = 0.05$. GUS staining **B)** and activity **C)** of DR5:GUS Dex:MKK10-2 (genetic crossing of DR5:GUS and Dex:MKK10-2) plants. Seedlings of 2 d after germination were treated with 10 μM Dex or DMSO for 6 (a) and 24 h (b). DR5:GUS Dex:MKK10-2 seedlings of 5 d old were treated with DMSO solvent or Dex for 12 h for GUS staining (c) and activity determination ($n = 14$) **C)**. DR5:GUS for auxin responsive elements (DR5) controlled *GUS* reporter gene; Bar = 1 cm. **D)** Expression of auxin related genes. Dex:MKK10-2 seedlings of 12 d old were treated with 10 μM Dex for 6 h and DMSO as the mock, and the leaves were sampled for total RNA isolation. Gene expression was determined by RT-qPCR using *OsUBQ* as the reference gene. Results from representative experiments are shown. Experiments were repeated three times with similar results. Values are means ± SD with significant difference compared with DMSO mock using Student's *t*-test (*, $P < 0.05$; **, $P < 0.01$; ***, $P < 0.001$).

highly inhibited with increased Dex concentration (Supplemental Fig. S8, A to C), suggesting that the elevation of *OsMKK10-2* expression was responsible for these phenotypes. Furthermore, the inhibition of root growth in Dex:MKK10-2-myc plants was attenuated under *w31ko* background in Dex:MKK10-2 *w31ko* (Supplemental Fig. S8, D and E), indicating that OsWRKY31 is an important regulator downstream of OsMKK10-2.

## Activation of OsMKK10-2 prioritizes defense responses over growth

As the activation of OsMKK10-2 promoted disease resistance and suppressed auxin transport and metabolism, we analyzed transcript levels of genes related to these phenotypes. Transcript levels of *OsMKK10-2* increased in different Dex:MKK10-2-myc plants by Dex treatment; however, the increased transcript levels of *OsMKK10-2* was slightly suppressed in *Dex:MKK10-2 w31ko* lines (Fig. 5A, Supplemental Fig. S9A). Activation of *OsMKK10-2* increased *OsWRKY31* expression in Dex:MKK10-2-myc. However, the level of *OsMKK10-2* transcript was not changed significantly in Ubi:fW31h plants, in which the level of *OsWRKY31* transcript was very high (Fig. 5B).

The jasmonic acid (JA)-inducible allene oxide synthase *OsAOS2*, a JA biosynthetic gene, was significantly induced by the activation of *OsMKK10-2* (Fig. 5C). *OsWRKY45* has been reported to play an important role in SA-mediated defense responses in rice (Shimono et al. 2007). The level of *OsWRKY45* transcript was upregulated approximately 3-fold in Dex:MKK10-2-myc plants, and this increase required functional *OsWRKY31* (Fig. 5D). Moreover, the expression of *OsPR1a* and *OsPR1b* was elevated in the Dex-induced OsMKK10-2 and Ubi:fW31h plants (Supplemental Fig. S5, E and F).

Overexpression of *OsPIN2*, which encodes an auxin efflux transporter of the PIN family, enhances auxin transport from shoots to roots (Chen et al. 2012). In our study, *OsPIN2* expression was strongly suppressed in Dex-induced Dex:MKK10-2-myc plants (Fig. 5G). Conversely, the expression of *OsAUX3*, belonging to the auxin influx carrier family, was elevated in Dex:MKK10-2-myc plants compared with the controls (Fig. 5H). Furthermore, the expression of *OsKS1*, leading to the synthesis of gibberellin (GA), was downregulated in Ubi:fW31h and Dex-induced Dex:MKK10-2-myc

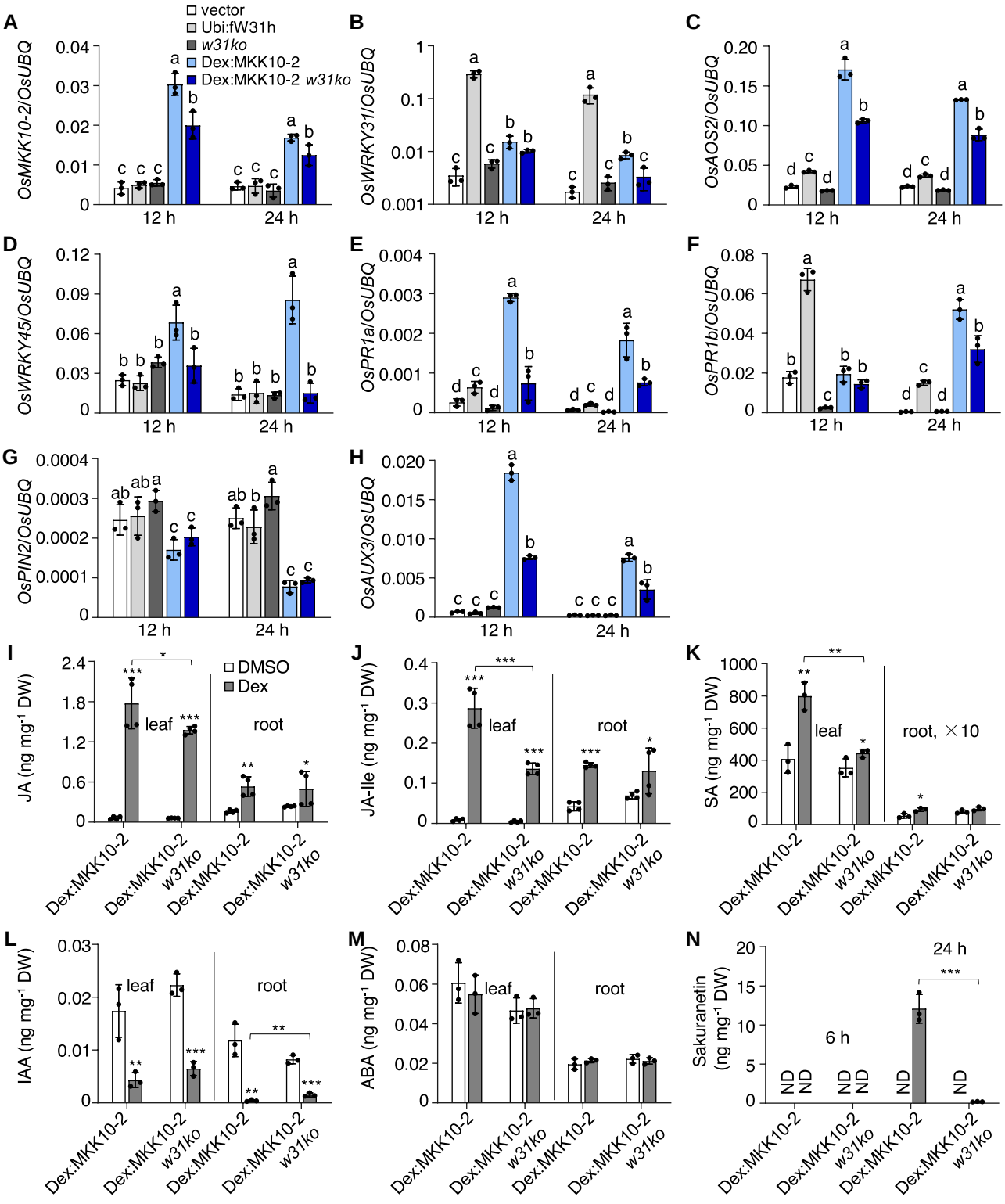


**Figure 5.** *OsWRKY31* is required for *OsMKK10-2*-activated immune response. The transgenic and control plants were hydroponically cultured for 10 d, treated with 10 μM Dex, and sampled at designated time points for RNA and chemical isolations. Transcript level of each gene **A** to **H)** was determined by RT-qPCR using *OsUBQ* as the internal reference. Values represent means ± SD of three indepent treatments, each including three seedling leaves. Values marked with different letters indicate statistically significant differences as analyzed by the SPSS software (Duncan's multiple range test, $\alpha = 0.05$). **I** to **N)** Contents of compounds were determined by liquid chromatography–tandem mass spectrometry using $D_6$ABA as the internal standard. **I** to **M)** sampled at 6 h after the Dex treatment. **N)** Leaf samples at 6 and 24 h after the Dex treatment; ND, no detection; root × 10, indicating 10 times upscale the value in root. Data are means ± SD of three or four biological repeats. Significance test was evaluated using the Student's *t*-test by comparing with DMSO treatment or each other as bracketed (*, $P < 0.05$; **, $P < 0.01$; ***, $P < 0.001$).

plants, whereas *OsKS4*, leading to synthesis of phytoalexin momilactones, was upregulated (Supplemental Fig. S9B). Increased *OsWRKY11* and *OsGH3.8* expression led to growth retardation and enhanced disease resistance (Ding et al. 2008; Cai et al. 2014). Transcript levels of both *OsWRKY11* and *OsGH3.8* genes were also upregulated in Ubi:fW31h and Dex-treated Dex:MKK10-2-myc plants (Supplemental Fig. S9B).

Hormonal profiling revealed that the accumulation of JA, jasmonoyl isoleucine (JA-Ile), and SA was remarkably elevated in both leaves and roots of Dex-treated Dex:MKK10-2-myc and, to a lesser extent, in Dex:MKK10-2 *w31ko* plants (Fig. 5, I to K). In contrast, IAA content in both roots and leaves decreased significantly by the induction of *OsMKK10-2* expression (Fig. 5L) but without noticeable changes in abscisic acid (ABA) accumulation (Supplemental Fig. S5M). The levels of the phytoalexin sakuranetin were highly increased in Dex:MKK10-2-myc leaves 24 h after Dex treatment; however, this induction was insignificant in Dex:MKK10-2 *w31ko* plants (Fig. 5N). We also examined phytohormone accumulation in *mkk10-2ko*, *w31ko*, and Ubi:fW31h plants with or without the inoculation of rice blast fungus. Contents of SA, JA, and JA-Ile were lower in the leaves of *mkk10-2ko* and *w31ko* mutants compared with Ubi:fW31h#2 and ZH17, although induction of JA and JA-Ile was still observed (Supplemental Fig. S10). SA content was not changed largely by *M. oryzae* challenge, consistent with the previous report (Yang et al. 2004). Collectively, the results suggest that activation of OsMKK10-2 promoted defense responses with a synergistic increase of SA and JA accumulation and suppressed auxin-related plant growth.

## OsMKK10-2 and OsWRKY31 participate in PAMP regulation of defense and auxin pathways

OsPIN2 mediates auxin distribution and plays an important role in root development and system architecture in rice (Wang et al. 2018). We examined the response of OsPIN2pro:GUS to chitin and verified that GUS staining was weakened at the lateral root primordia and root tips upon chitin treatment (Fig. 6A). Meanwhile, the number of the lateral root primordia was reduced by chitin treatment. Tests on basipetal PAT revealed a significant inhibition of PAT in rice seedlings in the presence of chitin or flg22 (Fig. 6B). Gene expression analysis revealed a downregulation of *OsPIN2* and upregulation of *OsGH3.8* in rice seedlings by chitin (Supplemental Fig. S11, C and D), consistent with the decrease of free IAA and suppression of its translocation by chitin. Expressions of *OsMKK10-2* and *OsWRKY31* were induced by chitin treatments, and notably, the chitin-induced defense-related *OsPR1b* and *OsKS4* expressions were substantially compromised in the *mkk10-2ko* and *w31ko* lines (Supplemental Fig. S11, A, B, E, and F).

As the activation of OsMKK10-2 promoted the accumulation of JA and SA and decreased IAA content (Fig. 5), we investigated the effects of methyl jasmonate (MeJA) and SA on auxin responses using OsPIN2pro:GUS and DR5:GUS plants. Histochemical assays of OsPIN2pro:GUS revealed that the GUS signal was significantly suppressed at the tips of primary roots by SA and MeJA treatments with or without IAA (Fig. 6C). Similarly, GUS activities of DR5:GUS and DR5:GUS *w31ko* were inhibited by SA and MeJA treatments (Fig. 6D), suggesting that SA and MeJA antagonize auxin effects. Analysis of gene expression revealed that *OsPIN2* expression in both roots and leaves is suppressed by the exogenous application of MeJA and SA, even in the presence of IAA (Fig. 6E, Supplemental Fig. S12). Conversely, IAA treatment inhibited the expressions of the MeJA-inducible marker gene *OsLOX2* and SA-inducible gene *OsWRKY76*. These findings suggest that PAMPs triggered immunity recruits OsMKK10-2 and OsWRKY31 to enhance defense reactions, and auxin pathway antagonizes with JA and SA pathways in rice plants.

## Phosphomimetic OsWRKY31 enhances *cis*-element-binding activity and disease resistance

We adopted an in vitro mutation approach to localize potential phosphorylation sites of OsWRKY31. Some of the Ser/Thr residuals of Ser/Thr-Pro loci—potential MAP kinase phosphorylation sites—in OsWRKY31 were mutated to Ala to produce non-phosphorylatable variants of the sites. OsWRKY31 and its mutants were subjected to phosphorylation assays by the interacting MPKs, and $Ser^{6}$ and $Ser^{101}$ residues were found as the major phosphorylation sites of OsMPK3, OsMPK4, or OsMKK10-2-activated OsMPK6 (Supplemental Fig. S13).

To investigate whether OsWRKY31 phosphorylation could affect its W-box-binding capability, we tested OsWRKY31 binding with probes of various combinations of W-box elements by electrophoretic mobility shift assays (EMSA). The recombinant OsWRKY31 protein interacted specifically with the probes from the promoter of *OsPR1b* with different affinity; however, OsWRKY31 contained a hepta WRKYGEK instead of the more conserved WRKYGQK motif in most of WRKY TFs (Supplemental Fig. S14A) (Chen et al. 2019). OsWRKY31 showed weaker binding to BP22-f1 (containing the core sequence TGAC of W-box) than BP22-f3 (containing TTGAC) probe, suggesting that OsWRKY31 might prefer to interact with the full W-box elements. Moreover, the phosphomimetic $OsWRKY31^{S6DS101D}$ protein showed stronger intensity of the retarded bands compared with those of OsWRKY31, whereas the phosphonull $OsWRKY31^{S6A}$ and $OsWRKY31^{S6AS101A}$ diminished markedly in the binding activity compared with the wild-type protein (Fig. 7, A and B, Supplemental Fig. S14B). Transactivation activity of OsWRKY31 and its phosphomutants was tested by using Wbox:GUS reporter in *N. benthamiana* leaves. A steady increase of relative activity was observed using OsWRKY31 and $OsWRKY31^{S6DS101D}$ effectors compared with $OsWRKY31^{S6AS101A}$ or the GFP control (Fig. 7, C and D), and the activity was increased by additional chitin treatment (Fig. 7E), which might increase OsWRKY31

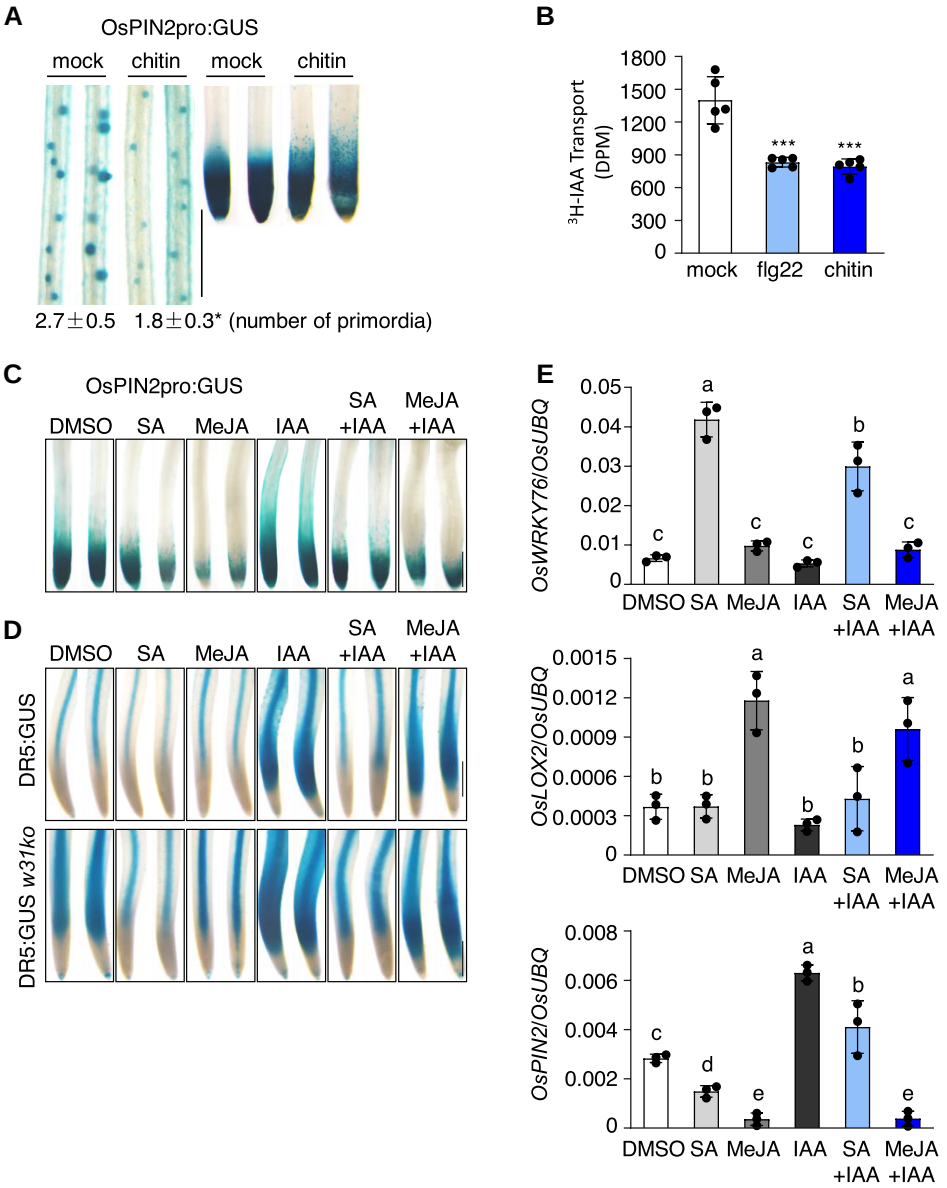


**Figure 6.** *OsMKK10-2* and *OsWRKY31* are involved in PAMP regulation of defense and auxin pathways. **A)** Changes of *OsPIN2pro:GUS* expression pattern and primordia formation by chitin treatment. Five-day-old OsPIN2pro:GUS seedlings were treated with 200 μg $mL^{-1}$ chitin for 12 h and stained at 37 °C for 4 h. Values are means ± SD of three biological replicates. **B)** Chitin and flg22 suppress auxin transport. Seven-day-old ZH17 seedlings grown in the dark were treated with 1 μM flg22 or 200 μg $mL^{-1}$ chitin for 12 h, and then the coleoptiles were collected for PAT assay as described in Fig. 4. Error bars represent standard deviation of five replicate experiments. Significance test was evaluated using the Student's *t*-test (***, $P < 0.001$). Suppression of *OsPIN2* **C)** and *DR5* **D)** promoter activities by MeJA and SA. Five-day-old OsPIN2pro:GUS, DR5:GUS, and DR5:GUS *w31ko* seedlings were treated with MeJA (200 μM), SA (500 μM), or in combination with IAA (1 μM), and the mock received the same amount of DMSO at 28 °C for 12 h. Representative GUS staining images of OsPIN2pro:GUS primary roots stained at 37 °C for 4 h, and DR5:GUS and DR5:GUS *w31ko* staining at 37 °C for 1 h. Bar = 0.5 mm **C** and **D)**. **E)** Expression of SA (*OsWRKY76*), JA (*OsLOX2*), and IAA (*OsPIN2*) marker genes in roots. Five-day-old DR5:GUS seedlings were treated with phytohormones as described in **D)**. Gene expression was determined by RT-qPCR analysis using *OsUBQ* as the reference. Data are means ± SD of three independent treatments. Values marked with different letters indicate statistically significant differences as analyzed by the SPSS software (Duncan's multiple range test, $\alpha = 0.05$).

and its phosphorylation levels with chitin application (see Fig. 8, A and B). The data indicated that OsWRKY31 is a transactivator.

To investigate the effects of OsWRKY31 phophosites *in planta*, we generated *OsWRKY31* phosphomimetic and phosphonull plants in the *w31ko#14* genetic background (Ubi:$W31^{S6DS101D}$-3flag *w31ko* and Ubi:$W31^{S6AS101A}$-3flag *w31ko*; abbreviated $W31^{DD}$-3flag *w31ko* and $W31^{AA}$-3flag *w31ko*, respectively). The phosphomimetic $W31^{DD}$-3flag *w31ko* plants presented a markedly increased resistance

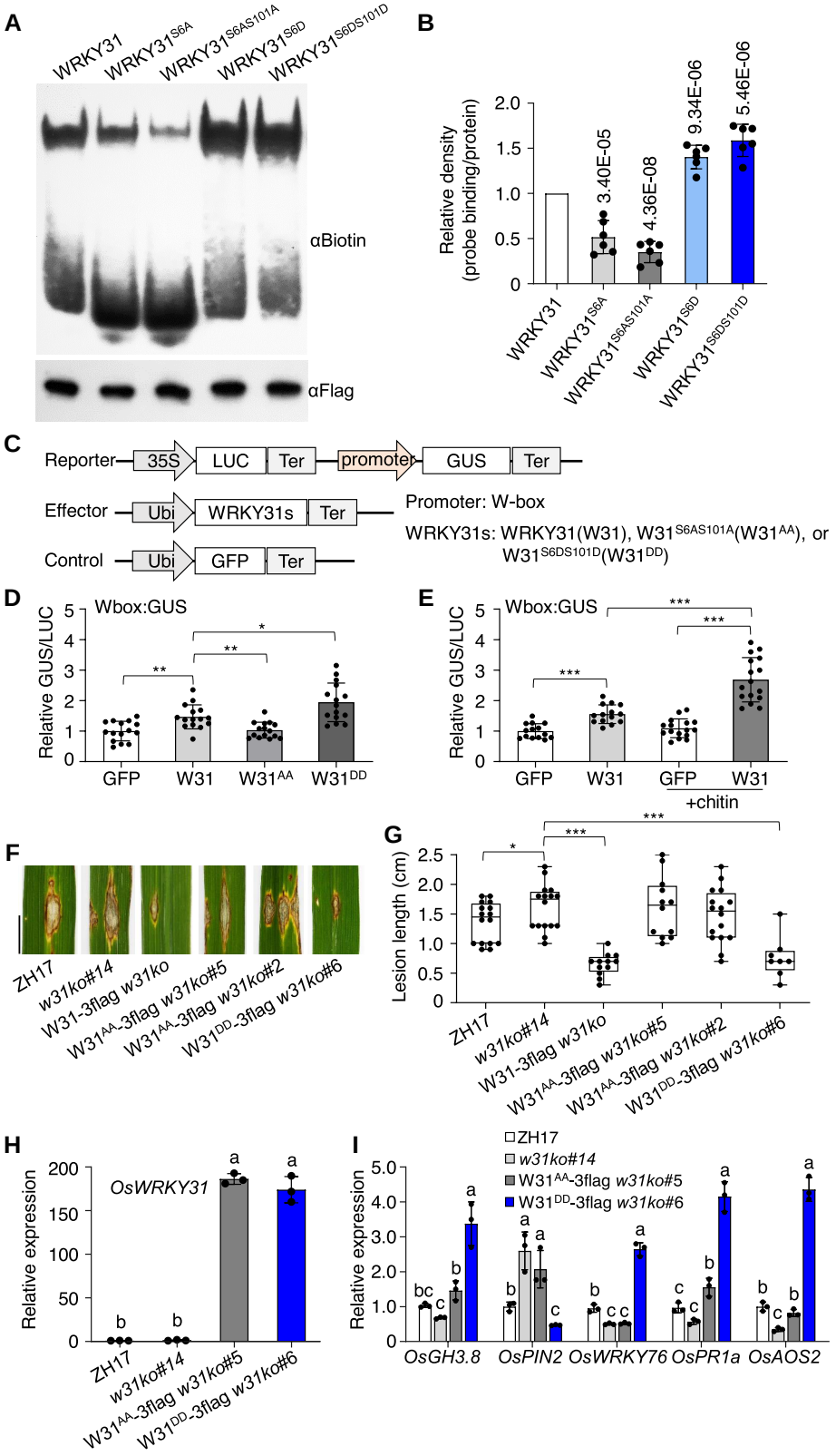


**Figure 7.** Phosphomimetic OsWRKY31 enhances DNA-binding activity and disease resistance. **A)** Phosphomimetic (GST-WRKY31$^{S6D}$-3flag and GST-WRKY31$^{S6DS101D}$-3flag), phosphonull (GST-WRKY31$^{S6A}$-3flag and GST-WRKY31$^{S6AS101A}$-3flag), and GST-WRKY31-3flag protein were expressed in *E. coli*. and purified for electrophoretic mobility shift assay using BP22-f3 probe (biotin-labeled P22-f3 probe, Supplemental Fig. S14A). The mixture

(continued)

against *M. oryzae* in comparison with W31$^{AA}$-3flag *w31ko*, *w31ko*, and ZH17 (Fig. 7, F and G, Supplemental Fig. S14, C and D). Expression of defense-related genes, *OsGH3.8*, *OsPIN2*, *OsWRKY76*, *OsPR1a*, and *OsAOS2*, was upregulated in W31$^{DD}$-3flag *w31ko*, whereas *OsPIN2* expression was suppressed (Fig. 7I). The transcript levels of defense-related genes were similarly much lower in phosphonull W31$^{AA}$-3flag *w31ko* and *w31ko* plants than in W31$^{DD}$-3flag *w31ko* lines, although both of the transgene *W31$^{AA}$-3flag* and *W31$^{DD}$-3flag* were highly expressed (Fig. 7, H and I). The observations indicated that the two phosphosites of OsWRKY31 are essential for its role in activation of disease resistance.

## Rapid induction of OsWRKY31 protein by chitin and *M. oryzae*

When the abundance of OsWRKY31 protein was examined, we found that the level of OsWRKY31 accumulation was low in Ubi:fW31h plants compared to the very high transcript levels of *OsWRKY31*, especially in hydroponic culture conditions (Fig. 5B). Rapid and transient induction of OsWRKY31 protein was observed in Ubi:fW31h plants treated with chitin (Fig. 8A). Similar to chitin treatment, the levels of OsWRKY31 protein and its phosphorylation were simultaneously elevated in Ubi:fW31h#2 plants treated with MG132, an inhibitor of proteasome-mediated protein degradation (Fig. 8B), suggesting that OsWRKY31 protein is regulated by the ubiquitin–proteasome system.

To address why W31$^{DD}$-3flag *w31ko* and W31-3flag *w31ko* lines showed similar levels of resistance against *M. oryzae* (Fig. 7, F and G), we analyzed the levels of the proteins encoded by the respective transgenes. The abundance of the phosphomimetic mutant OsWRKY31$^{DD}$ was higher than wild-type OsWRKY31 revealed by comparing the samples (0 h) before the pathogen infection (Fig. 8C) and among different transgenic lines (Supplemental Fig. S14D). OsWRKY31 abundance was markedly elevated after inoculation of *M. oryzae* SZ strain in 3 h, a very early infection period for the pathogen infection, and reached to the level of OsWRKY31$^{DD}$ (Fig. 8C). The results imply that the rapid induction of OsWRKY31 protein is able to compensate for the lower level at the beginning than OsWRKY31$^{DD}$, and also the phosphorylated OsWRKY31 is more stable than its wild type (Figs. 2C and 8B).

To further confirm the relationship between OsWRKY31 abundance and its phosphorylation status, we transiently expressed OsWRKY31 with OsMPK3 in *N. benthamiana* leaves via agroinfiltration. The levels of OsWRKY31 protein and its phosphorylation were higher in plants expressing Ubi:W31-3flag with 35S:MPK3-myc than with 35S:MPK3$^{KR}$-myc or 35S:GFP-myc (Fig. 8D), supporting the idea that OsWRKY31 phosphorylation favors its protein accumulation and is consistent with that observed in Fig. 2C. The increased OsWRKY31 could be because an increase of phosphorylated active OsWRKY31 triggers a large variation in defense signaling and stimulates a higher level of expression of unphosphorylated OsWRKY31. Collectively, the rapid induction of OsWRKY31 accumulation by chitin and during the early infection of rice blast fungus suggested that OsWRKY31 is highly controlled for efficient defense responses.

## OsWRKY31 stability is regulated by ubiquitination

Since OsWRKY31 stability is mediated by the proteasome system, we searched E3 ubiquitin ligases as potential interactors of OsWRKY31. A RING-finger E3 ubiquitin ligase interacting with WRKY, designated as OsREIW1, was previously obtained through a Y2H screen. By transcriptomic analyses of plant responses to a panel of phytohormone treatments (Sato et al. 2013), we found that *OsREIW1* is co-regulated with *OsWRKY31* (Supplemental Fig. S15A). Further, OsWRKY31 was verified to interact with OsREIW1 protein, but not the E3 ligase PUB6 in yeast cells and by pull-down experiment (Fig. 9, A and B). Interaction of OsWRKY31

**Figure 7.** (Continued)
of protein (about 2 μg) with probe (0.03 μM) was separated on native PAGE gels and detected with αBiotin antibody. The presence of retarded band indicating the formation of protein–DNA complex. Protein loading was analyzed using αFlag antibody. **B)** The relative density is the retarded band in related to the loading protein and normalized with the wild-type OsWRKY31 protein. Values are means ± SD of six repeats. *P*-values are shown in the graph. **C)** Schematic diagrams of the reporter and effector constructs. The promoter was fused with *GUS* reporter gene. *LUC* gene driven by the cauliflower mosaic virus (CaMV) 35S was used as an internal control. The W-box DNA was put ahead of 35S minimal promoter with TATA-box to generate Wbox:GUS construct. **D** and **E)** Effector of OsWRKY31 (W31), phosphomimetic OsWRKY31$^{S6DS101D}$ (W31$^{DD}$), phosphonull OsWRKY31$^{S6AS101A}$ (W31$^{AA}$), or GFP control was co-infiltrated with the reporter of Wbox:GUS in the leaves of *N. benthamiana*. The treated tobacco plants were grown 25 °C for 3 d and sampled for GUS activity. In case of chitin treatment, the leaves were sprayed with chitin solution (200 μg mL$^{-1}$) 5 h before the sample collection. Values are means ± SD of different leaf discs ($n \geq 14$). Overexpression of phosphomimetic *OsWRKY31$^{DD}$* elevated resistance to *M. oryzae* SZ strain. **F** and **G)** The phosphomimetic *W31$^{DD}$-3flag*, the phosphonull *W31$^{AA}$-3flag*, and *W31-3flag* genes (all controlled by ubiquitin promoter) were transformed into *w31ko* background. The hygromycin-resistant transgenics of $T_2$ progenies and the ZH17 control were grown to the tillering stage in the paddy filed and inoculated with spores of *M. oryzae* SZ ($1 \times 10^5$ conidia mL$^{-1}$) in year 2020. The leaf segments were photographed and quantified at 9 d after the infiltrations. The median was the crossline in each boxplot showing the lesion length distributions ($n \geq 8$). Significance was evaluated by comparing with each other as bracketed using the Student's *t*-test (*, $P < 0.05$; **, $P < 0.01$; ***, $P < 0.001$). Bar = 1 cm. **H** and **I)** Gene expression. Leaves of 10-d-old seedlings cultured hydroponically were used for total RNA isolation. Gene expression was determined by RT-qPCR using *OsUBQ* as the reference gene. Values are means ± SD of three independent expereiments, each including three seedling leaves. Values marked with different letters indicate statistically significant differences as analyzed by the SPSS software (Duncan's multiple range test, $\alpha = 0.05$).

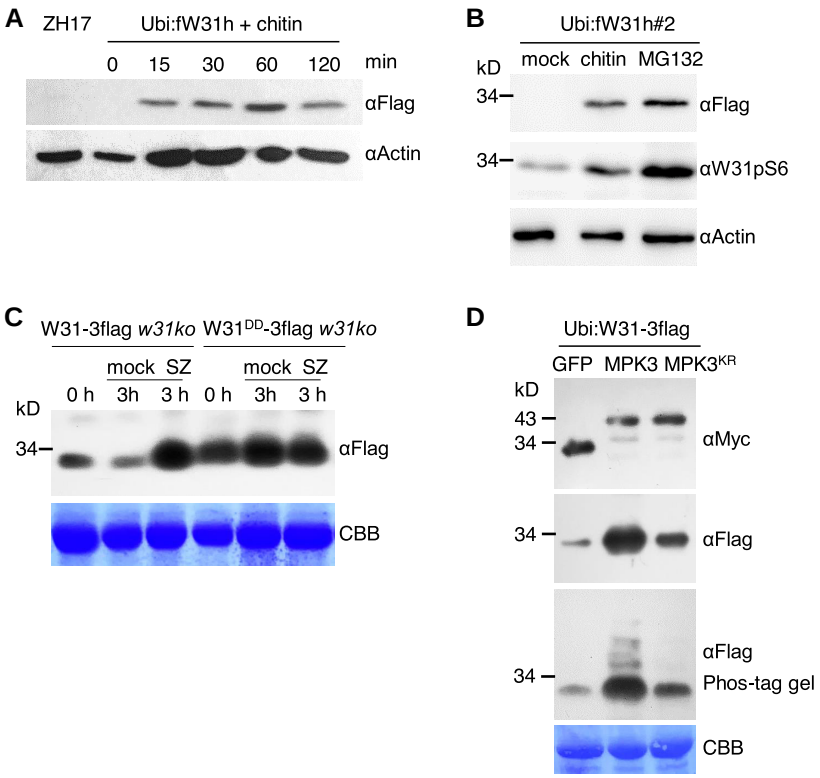


**Figure 8.** Rapid induction of OsWRKY31 protein by chitin and *M. oryzae*. **A** and **B)** Induction of OsWRKY31 accumulation by chitin and proteasome inhibitor MG132. Leaves of 7-d-old Ubi:fW31h#2 were treated with 200 μg $mL^{-1}$ chitin, 100 μM MG132 or DMSO as the mock for 1 h **B)** or with 200 μg $mL^{-1}$ chitin at various time points **A)**. The extracted proteins were analyzed by immunoblots with antibodies of αFlag, αW31pS6, and αActin as the loading control. **C)** Induction of OsWRKY31 protein by *M. oryzae*. Eighteen-day-old rice plants (Ubi:$W31^{DD}$-3flag *w31ko* and Ubi:W31-3flag *w31ko*) growing in soil were inoculated with spores of *M. oryzae* SZ ($5 \times 10^5$ conidia $mL^{-1}$) by spraying, and the leaves were sampled for protein analysis at 3 h after or before (0 h) the challenge. The proteins extracted were analyzed by immunoblots with αFlag antibody. Results from representative experiments are shown. Experiments were performed in three replicates. **D)** Increase OsWRKY31 accumulation by phosphorylation. Agrobacteria harboring Ubi:W31-3flag plasmid were co-infiltrated with agrobacteria containing 35S:MPK3-myc, 35S:$MPK3^{KR}$-myc, or 35S:GFP-myc, into the leaves of *N. benthamiana*. Proteins were extracted from the leaves of 2 d after the infiltrations and analyzed by immunoblots with αMyc and αFlag antibodies. CBB, Coomassie brilliant blue staining for loading control. Representative data from three independent experiments.

with $OsREIW1^{H56Y}$ ($His^{56}$ to Tyr, to eliminate the enzymatic activity) mutant was mainly in the nucleus of *N. benthamiana* leaves by BiFC assay (Fig. 9C), supported by the predominant localization of both OsREIW1 and OsWRKY31 in the nuclei (Supplemental Fig. S15B) (Zhang et al. 2008).

Recombinant GST-REIW1-3myc protein exhibited self-ubiquitination activity, and the $OsREIW1^{H56Y}$ mutant showed no enzymatic activity (Supplemental Fig. S15C). OsWRKY31 was highly ubiquitinated by OsREIW1 (Fig. 9D). In contrast, ubiquitination of the phosphomimetic $OsWRKY31^{DD}$ was weaker than the phosphonull $OsWRKY31^{AA}$ and OsWRKY31 (Fig. 9D), implying that phosphorylation of OsWRKY31 at the two sites potentially attenuates the ubiquitination and increases the protein stability. This note is consistent with the higher level of $OsWRKY31^{DD}$ in its transgenic plants compared to OsWRKY31 plants (Fig. 8C, 0 h).

Moreover, we used a cell-free approach to compare the stability of OsWRKY31 and $OsWRKY31^{DD}$ during incubation with protein extracts from *OsREIW1*-overexpressing plants. GST-$WRKY31^{DD}$-3flag showed slower degradation than GST-WRKY31-3flag (Supplemental Fig. S15D). Compared with *OsREIW1* knockout (*reiw1ko*) plants, GST-WRKY31-3flag degradation was faster in the extracts from *OsREIW1*-overexpressing or wild-type ZH17 plants (Fig. 9, E and F). Lower OsWRKY31 abundance was detected in Ubi:fW31h Ubi:REIW1 plants (Ubi:fW31h and Ubi:REIW1-3myc cross progeny) than in Ubi:fW31h *reiw1ko* plants (Fig. 9G). Notably, OsWRKY31 levels in Ubi:REIW1-3myc plants but not in *reiw1ko* plants were increased upon MG132 treatment (Fig. 9G), suggesting that OsWRKY31 is a target of OsREIW1 for degradation via 26S proteasome.

The *OsREIW1*-related plants were tested for the response to *M. oryzae* SZ. The knockout mutant of *OsREIW1* exhibited enhanced resistance against the fungal pathogen, whereas Ubi:REIW1-3myc plants were more susceptible to the SZ pathogen than ZH17 (Fig. 9, H and I). The elevated resistance in Ubi:fW31h plants was compromised in the presence of Ubi:REIW1-3myc, indicating that OsREIW1 is a negative

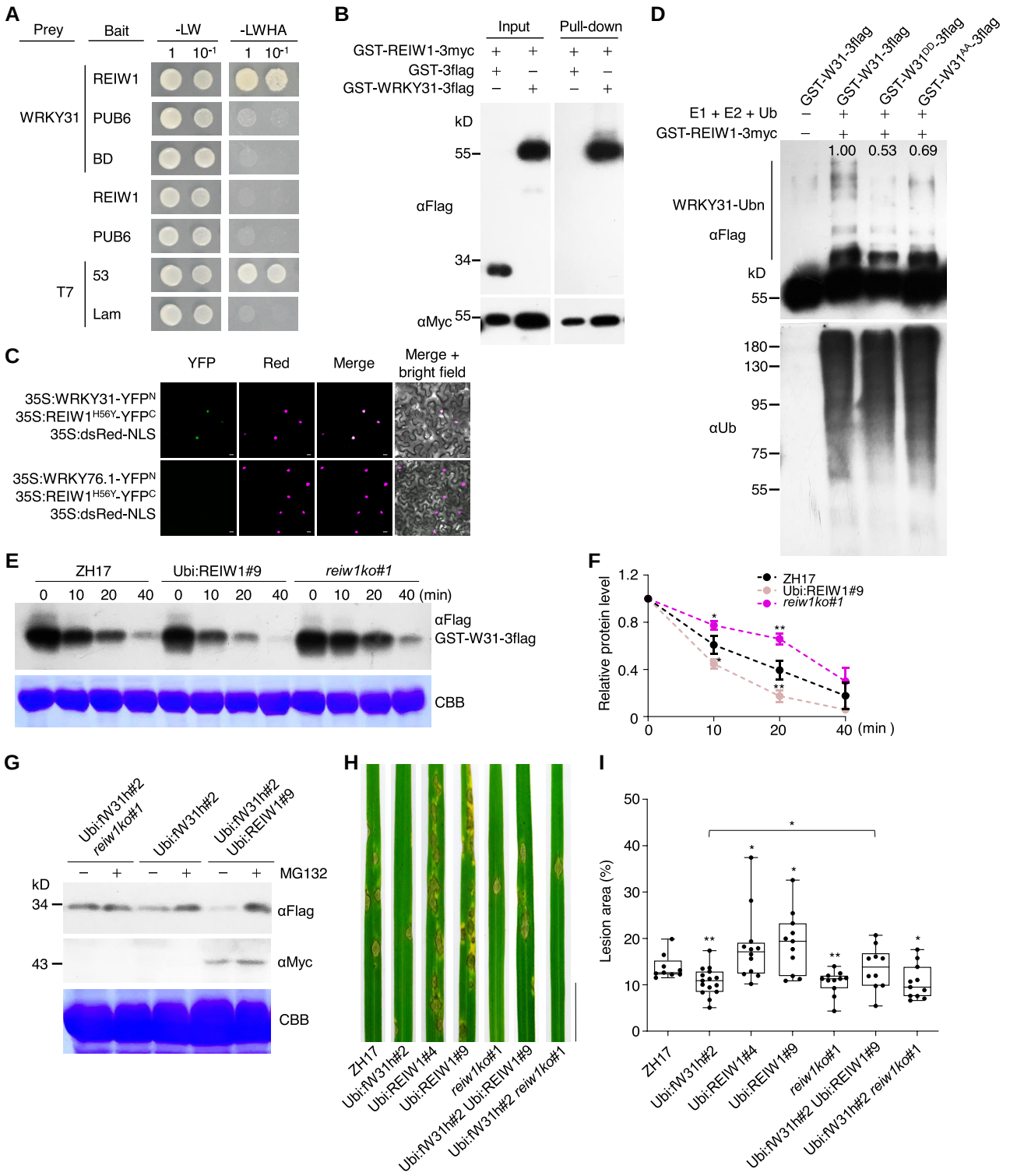


**Figure 9.** OsREIW1 regulates OsWRKY31 stability. **A** to **C)** OsREIW1 interacts with OsWRKY31. **A)** OsREIW1 and PUB6 as a control were fused to the Gal4 DNA-binding domain (bait). The prey-OsWRKY31 was from Fig. 1. Yeast cells were incubated in SD medium without Leu and Trp (-LW) or lacking Leu, Trp, His, and adenine (-LWHA), and photographed 3 d after plating. Yeast cells containing AD-T7 plus BD-53 and AD-T7 plus BD-Lam plasmids were used as the positive and negative controls, respectively. **B)** Purified GST-REIW1-3myc and GST-WRKY31-3flag protein (each about 1 μg) were mixed and incubated at 4 °C for 2 h in immunoprecipitation buffer. The protein mixture was precipitated with anti-c-Myc agarose affinity gels, separated on 10% SDS-PAGE gels, and detected by immunoblots with αMyc and αFlag antibodies. **C)** Agrobacteria harboring 35S:REIW1$^{H56Y}$-YFP$^{C}$, 35S:WRKY31-YFP$^{N}$ or 35S:WRKY76.1-YFP$^{N}$ plasmid were combined accordingly and infiltrated into the leaves of *N. benthamiana*.

(continued)

regulator of *OsWRKY31*-mediated defense responses. Collectively, these findings demonstrated that OsWRKY31 stability is regulated by phosphorylation and ubiquitination.

## Discussion

In this study, we provided evidence that OsWRKY31 is a key regulator of rice defense and growth, acting downstream of OsMKK10-2 in a OsMKK10-2–OsMPK3–OsWRKY31 cascade. In addition, we found that OsWRKY31 stability is regulated by phosphorylation and ubiquitination via a RING-finger E3 ligase, OsREIW1.

### OsMKK10-2–OsMPK3/6 activates OsWRKY31 in rice immunity

In the MPK cascades, OsMKK10-2 has been shown to interact directly or indirectly with environmental stress-related OsMPK3, OsMPK4, and OsMPK6 (Ueno et al. 2015; Ma et al. 2017; Zhou et al. 2017). Ueno et al. (2013, 2015) have addressed the OsMKK10-2–OsMPK6–OsWRKY45 pathway in *M. oryzae* resistance, in which ABA treatment leads to dephosphorylation of OsMPK6 via activation of protein tyrosine phosphatases and improves disease resistance. Thus, OsMKK10-2–OsMPK3–OsWRKY45 appears to mediate SA–ABA signaling crosstalk between disease-resistance and abiotic-stress responses. Similarly, Ma et al. (2017) have shown that overexpressing *OsMKK10-2* increases resistance to the bacterial pathogen *Xoc* and tolerance to drought, whereas its RNAi-knockdown plants are more sensitive to *Xoc* and drought stress compared with the control plants. The disease-resistance and drought-tolerance pathways are regulated separately by OsMKK10-2–OsMPK6 and OsMKK10-2–OsMPK3 modules, respectively (Ma et al. 2017). In this study, we showed that activation of OsMKK10-2–OsMPK3–OsWRKY31 promotes defensive responses and this particular signaling cascade has a negative effect on auxin-related activities including downregulation of genes for auxin biosynthesis, signaling, and transportation (Figs. 3 to 5). These results point to an involvement of OsMKK10-2–OsMPK3-OsWRKY31 in SA–IAA signaling crosstalk. We find it interesting that both OsMKK10-2–OsMPK6–OsWRKY45 and OsMKK10-2–OsMPK3–OsWRKY31 cascades regulate rice defense but have negative crosstalk with ABA (in the case of OsWRKY45) or auxin (in the case of OsWRKY31) hormonal pathways. Likely, OsWRKY31 is involving defense and auxin, whereas OsWRKY45 participated in defense and ABA signaling. Future research is needed to further examine if OsWRKY31 and OsWRKY45 have nonredundant and/or overlapping roles in mediating other aspects of defense-growth trade-offs. Phylogenetically, OsWRKY45 belongs to the WRKY IIIa subclade, whereas OsWRKY31 is in the IIIb subclade. These two subclades appear to have evolved after the divergence of dicots and monocots (Wu et al. 2005).

Furthermore, we found the formation of OsMKK10-2–OsMPK3–OsWRKY31 ternary complex (Fig. 1E), which potentially increases the efficiency of OsWRKY31 phosphorylation and specificity of the signaling pathway. The protein complex is often observed in the metabolic channeling, which allows an efficient control of metabolic flux (Achnine et al. 2004). The complex of LOX2, AOS2, and AOC2 in the plastid envelope of *Arabidopsis* chloroplasts provides a channel for JA precursor biosynthesis (Pollmann et al. 2019). In *Arabidopsis*, MEKK1 interacts with and directly phosphorylates WRKY53 and regulates *WRKY53* through binding to its promoter, suggesting that MEKK1 can act as a short cut in MPK signaling (Miao et al. 2007). However, the biochemical function associated with the interaction between OsMKK10-2 and OsWRKY31 is yet to be clarified.

### OsMKK10-2 and OsWRKY31 mediate the defense and growth trade-off

PAMPs, such as flg22, have been demonstrated to repress auxin signaling in *Arabidopsis* (Navarro et al. 2006). Our results showed that chitin inhibited IAA transport in rice seedlings and downregulated *OsPIN2* expression (Supplemental

**Figure 9.** (Continued)
Confocal images were taken at 2 d after the infiltrations. Red fluorescence signals indicative of the nuclei were from co-infiltrated 35S:dsRed-NLS (NLS: nuclear localization signal). Bar = 10 μm. **D)** Ubiquitination of OsWRKY31 by OsREIW1. OsWRKY31 recombinant protein GST-W31-3flag and its phosphomimetic GST-W31$^{DD}$-3flag and phosphonull GST-W31$^{AA}$-3flag were incubated with E1, E2, and ubiquitin in the presence of GST-REIW1-3myc. The reaction mixture (30 μL) contained 50 ng wheat ubiquitin-activating enzyme E1, 100 ng human ubiquitin-binding enzyme E2 (UBCH5b), 5 μg *Arabidopsis* ubiquitin (Ub), 500 ng GST-REIW1-3myc, and 2 μg OsWRKY31 or its mutant protein in buffer (50 mM Tris-HCl pH 7.5, 10 mM $MgCl_2$, 2 mM DTT, and 5 mM ATP) and incubated at 30 °C for 1 h. The reaction was stopped by adding the 5× SDS loading buffer. Samples were separated by 10% SDS-PAGE gels and analyzed by immunoblots using αUb or αFlag antibody. Relative intensity (numbers in the gel) of ubiquitinated bands was analyzed using ImageJ software. **E** and **F)** Cell-free degradation of OsWRKY31. Total proteins were extracted from the leaves of Ubi:REIW1-3myc, *reiw1ko*, and ZH17 seedlings grown hydroponically for 1 wk. Protein extracts (about 500 μg) were incubated with GST-WRKY31-3flag (2 μg) for various time points at 25 °C. The protein samples were separated and analyzed by immunoblot with αFlag antibody. Representative data from three independent experiments. Quantification of treatments at 0 min was set as 1. Values are mean ± SD ($n = 3$). **G)** Segments of leaves from 7-d-old seedlings cultured hydroponically were treated with 100 μM MG132 or DMSO solvent for 1 h and then sampled for protein isolation. The protein mixture was separated on 10% SDS-PAGE gels and detected by immunoblots with αMyc and αFlag antibodies. Representative results from three independent experiments. CBB, Coomassie brilliant blue staining for loading control. **H** and **I)** Eighteen-day-old plants were inoculated with *M. oryzae* SZ spores ($5 \times 10^5$ conidia $mL^{-1}$) by foliar spraying. Disease symptoms **H)** and lesion areas **I)** were conducted at 7 d after the inoculation. Representative data from three independent experiments. Significance was evaluated by comparing with ZH17 or each other as bracketed using Student's *t*-test (*, $P < 0.05$; **, $P < 0.01$). Bar = 2 cm.

Fig. S11C). GUS signal depletion in OsPIN2pro:GUS and DR5:GUS plants by the addition of SA or MeJA revealed the antagonistic effect of SA and MeJA on IAA in rice plants (Fig. 6, C to E). Activation of *OsMKK10-2* increased the levels of SA and JA/Ile-JA, whereas knockout of *OsWRKY31* compromised the induced phytohormnone accumulation (Fig. 5, I to K). This is consistent with the activation of *OsMKK10-2* or overexpressing *OsWRKY31* inhibiting root growth and enhancing resistance against *M. oryzae* (Supplemental Fig. S8, B and C; Zhang et al. 2008). The effects on growth and defense via *OsMKK10-2* are remarkably suppressed by knockout of *OsWRKY31* (Fig. 3, C and D, Supplemental Fig. S8, D and E), indicating that *OsWRKY31* is an important downstream component of *OsMKK10-2*. Additionally, OsWRKY31 possibly has a feedback effect on *OsMKK10-2* expression because *OsMKK10-2* expression is slightly suppressed in the *w31ko* background (Figs. 5A, Supplemental Fig. S9, A and S11A), but we cannot exclude the possibility of partial silencing of the DEX-induced *OsMKK10-2* in the *w31ko* background. Together, our data indicate that the OsMKK10-2–OsMPK3/6–OsWRKY31 module functions at a node for rice defense and growth, even though the study here was focused on the seedling stage, which may not reflect growth effects at the whole-plant scale.

## Role of OsMPK3 in rice resistance

We demonstrated, using a *mpk3ko* mutant, that OsMPK3 is an important kinase activated by OsMKK10-2 in defense response (Figs. 2B and 3, A to D), providing updated information on MPK signaling in rice. Knockout of *OsMPK3* only partially compromised *OsMKK10-2*-induced resistance to *M. oryzae* (Fig. 3D), suggesting that other kinases may have contributed to OsMKK10-2-mediated disease resistance, as OsMKK10-2 was able to phosphorylate several OsMPKs (Fig. 2B) (Zhou et al. 2017). Disease assays on *mpk3ko* mutants, Dex:MKK10-2 *mpk3ko* and Ubi:fW31h *mpk3ko* plants, suggested that OsMPK3 acts as a positive regulator of resistance against rice blast fungus, which differs from previous studies showing *OsMPK3* as a negative regulator (Xiong and Yang 2003; named as *OsMAPK5* therein). The phenotypic discrepancies between gene knockout and gene knockdown may be caused by a genetic compensation response, as noted in zebrafish (Rossi et al. 2015; Ma et al. 2019) and plants (Gao et al. 2015). Alternatively, the difference is possible due to cultivar variations and pathogens used in the studies.

## Phosphomimetic OsWRKY31 facilitates its DNA-binding activity

OsWRKY31 with a hepta WRKYGEK instead of the more conserved WRKYGQK motif shows binding activity to different combinations of W *cis*-elements (Supplemental Fig. S14A). Phosphorylation analyses in vitro demonstrated that OsWRKY31 could be phosphorylated directly by OsMPK3 and OsMPK4 but not OsMPK6 and that OsWRKY31 S6 and S101 are major phosphosites of the OsMPKs (Supplemental Fig. S13). Other studies have shown that MPKs can directly phosphorylate substrates in vitro. For instance, *Arabidopsis* MPK6 directly phosphorylates elFiso4G1, a component of the translational preinitiation complex and OsMPK3 phosphorylates SUB1A (Singh and Sinha 2016; Wang et al. 2022). We found that the phosphomimetic OsWRKY31$^{S6DS101D}$ facilitated W-box-binding and enhanced disease resistance against rice blast fungus, whereas the phosphonull OsWRKY31$^{S6AS101A}$ diminished W-box-binding activity (Fig. 7, A and B).

Phosphorylation-mediated effects on WRKY binding to target DNA have been reported previously. For example, *Arabidopsis* WRKY70 is able to bind the W-box for inhibition and WT-box for activation regulation (Liu et al. 2021). Phosphomimetic WRKY70 can still bind the WT-box but not the W-box. Phosphorylation of OsWRKY53 markedly enhances binding activity to a W-box-containing DNA sequence (Tian et al. 2017). Similarly, phosphomimetic MdWRKY17 elevates W-box binding, and its nonphosphorylatable mutant compromises the DNA-binding activity (Shan et al. 2021). Change of phosphorylation status may affect protein charges, conformation, and formation of homocomplexes, leading to alteration of DNA-binding activity. The results indicate that the selectivity and affinity of a WRKY TF towards variant W-boxes is influenced by its post-translational modification by phosphorylation (Chen et al. 2019; Liu et al. 2021).

## Phosphomimetic OsWRKY31 increases its stability

We found that degradation of OsWRKY31 is mediated by OsREIW1, a RING-finger ubiquitin E3 ligase, through the 26S proteasome (Fig. 9), likely explaining the low level of OsWRKY31 protein in OsWRKY31-overexpressing plants (Fig. 2C). Intriguingly, the phosphomimetic OsWRKY31$^{DD}$ seems more stable than the wild-type protein (Fig. 8D, Supplemental Fig. S14D), which is consistent with weaker ubiquitination in in vitro assays (Fig. 9D). Transcription regulators activated via phosphorylations are inclined to degrade in comparison with their native forms (Min et al. 2019; Liu et al. 2021). This on-and-off regulatory process can presumably avoid overdose responses to stimuli. Upregulation of defense-related genes in Ubi:W31$^{DD}$-3flag *w31ko* plants is consistent with the relatively high amount of OsWRKY31$^{DD}$ protein; however, levels of the increase in gene transcripts, such as *OsPR1a* and *OsAOS2*, are lower than those induced by activation *OsMKK10-2* at 12 h (Figs. 5, C and E and 7I), implying a restricted elevation of OsWRKY31$^{DD}$. Conversely, OsWRKY31 protein can be rapidly induced by chitin and *M. oryzae* (Figs. 2C and 8C), thereby promptly raising the defenses in *OsWRKY31*-overexpressing plants. Under chilling stress, OsbHLH002/OsICE1 is phosphorylated by OsMPK3, leading to inhibition of OsbHLH002 ubiquitination by the OsHOS1 E3 ligase and enhanced chilling tolerance (Zhang et al. 2017). Nevertheless, the stability of OsWRKY31$^{DD}$ needs further clarification. Based on our findings and those of previous studies, we

propose that OsMKK10-2 activated by biotic and abiotic stimuli phosphorylates OsMPKs that lead to the phosphorylation of TFs including OsWRKY31 to promote immunity; OsWRKY31 protein is controlled by phosphorylation and ubiquitination for fine-tuning the defense and growth balance.

## Materials and methods

### Plant growth and treatments

The seeds of wild-type (*O. sativa* L. ZH17) and transgenic plants were surface sterilized and germinated in 1/2 MS medium. The seedlings were transferred to 96-hole plates and cultured in 1/4 MS liquid medium at 28 °C under the white fluorescent light intensity of 200 μmol $m^{-2}$ $s^{-1}$ with a 12 h light/12 h dark photoperiod. Seedlings at designated age were treated with 5 mM MES (4-morpholineethanesulfonic acid, pH 5.8) buffer containing 500 μM SA, 200 μM MeJA, 1 μM flg22, or 200 μg $mL^{-1}$ chitin and used for RNA isolation or GUS activity.

To investigate the effect of OsMKK10-2 on seedling growth, the germinated seeds of Dex:MKK10-2-myc and ZH17 controls were transferred to 1/2 MS solid medium containing 0.24% [w/v] phytagel and various contents of Dex or the same amount volume of DMSO solvent as the mock treatment and grown at 28 °C for 5 d.

### Generation of transgenic plants

The coding sequences of *OsMKK10-2* and *OsREIW1* were amplified from ZH17 cDNA using gene specific primers (Supplemental Table S1, including all primers used in this study). OsMKK10-2$^{DD}$, OsWRKY31$^{S6AS101A}$, and OsWRKY31$^{S6DS101D}$ variants were generated by PCR-based site-directed mutagenesis. The sequence of *OsMKK10-2* was fused with one Myc tag at the 3′ end and put under the control of a Dex-inducible promoter to generate Dex:MKK10-2-myc. OsWRKY31$^{S6AS101A}$ and OsWRKY31$^{S6DS101D}$ were cloned to fuse with 3×Flag and controlled by the maize (*Zea mays*) *Ubiquitin* promoter, ligated into restriction endonuclease sites of *Bam*H I and *Pma*C I in a modified pCAMBIA1301 vector to generate Ubi:W31$^{AA}$-3flag and Ubi:W31$^{DD}$-3flag plasmids, respectively (Liu et al. 2016). Similarly, OsREIW1 was constructed as Ubi:REIW1-3myc. For CRISPR/Cas9 editing, the target sequence of each gene (Supplemental Table S1) was put under the control of the U3 promoter in pOsCas9 vector and verified by sequence. DR5:GUS vector was constructed by substitution of the W-box fragment in Wbox:GUS plasmid (Liu et al. 2016).

All of the plasmids constructed were verified by sequencing and introduced into *A. tumefaciens* EHA105 for rice transformation. The transgenic plants were generated from the immature seeds of ZH17 by the *Agrobacterium*-mediated transformation method (Hiei et al. 1994) unless indicated specifically. Ubi:W31$^{AA}$-3flag and Ubi:W31$^{DD}$-3flag plasmids were transformed into the immature seeds of *OsWRKY31* knockout (*w31ko#14*) segregant without the transferred CRISPR/Cas9 vector. Transgenic plants were analyzed by PCR amplification and the positive plants of $T_2$ or higher progeny were used in the experiments. Dex:MKK10-2 *w31ko*, Dex:MKK10-2 *mpk3ko*, and Ubi:fW31h *mkk10-2ko* were generated by genetic crossing.

### Pathogen inoculation

Eighteen-day-old rice plants, grown in soil containing peat moss and vermiculite (1:1), were inoculated with a virulent *M. oryzae* SZ strain by spraying the spore suspension ($5 \times 10^5$ conidia $mL^{-1}$ containing 0.005% [v/v] Silwet L-77) as described by Liu et al. (2016). In the case of Dex treatment required, 20 μM Dex solution containing 0.002% [v/v] Silwet L-77 was sprayed 12 h before the spore inoculation, whereas the mock treatment received the same amount of DMSO solvent. For injection of rice blast spores, rice plant after tillering (3-mo-old) was injected with the spores ($1 \times 10^5$ conidia $mL^{-1}$) to each leaf sheath at the bottom, and the newly grown leaves were collected for disease severity evaluation.

### Auxin transport assay

The sterilized seeds were grown in 1/2 MS liquid medium with 5 mM MES (pH 5.8) at 28 °C in the dark. Seven-day-old seedlings were treated with 200 μg $mL^{-1}$ chitin or 1 μM flg22 (in 5 mM MES, pH 5.8) for 12 h, and the seedlings harboring Dex:MKK10-2-myc construct were treated with 10 μM Dex for 12 h. The seedlings were segmented from 2 mm below the tip (20 mm length) and incubated in 1/2 MS medium with moderate shaking for 3 h to deprive endogenous IAA. A microdroplet of $^3$H-IAA (30 μL, 500 nM $^3$H-IAA and 500 nM unlabeled IAA in 1/2 MS medium containing 5 mM MES, pH 5.8) was applied to the apical tips at 28 °C for 3 h. Fifteen-millimeter segments from the other ends were harvested and quickly rinsed with 1/2 MS medium for three times. The samples were incubated in 3 mL scintillation fluid for 18 h and then used for radioactivity measurement on liquid scintillation counter (Perkin-Elmer, 1450 MicroBeta TriLux).

### Yeast two-hybrid assay

The DNA fragments of genes and their mutants were inserted into pGBKT7 or pGADT7 vector (Clontech) to generate bait or prey plasmid. Appropriate combinations of bait and prey constructs were transformed into yeast cells and then grown at 28 °C for 3 d on the synthetic dropout medium without Leu and Trp and the selection medium deficiency of Leu, Trp, His, and Ade for interaction test.

### Protein expression and purification

OsMKK10-2, OsMPK3, OsMPK4, OsMPK6, OsWRKY31, OsREIW1, and their mutants were cloned into a modified pGEX-tag vector, respectively (Liu et al. 2016), with 3×Myc or 3×Flag at the C-terminus of the recombinant protein. Each plasmid was transformed into *E. coli* BL21 (DE3), and

protein expression was induced by addition of 0.2 mM IPTG followed by incubation at 28 °C for 6 h. The recombinant proteins were purified using Glutathione Sepharose 4B (GE Healthcare).

## Pull-down assay

GST-MKK10-2-3myc, GST-MKK10-$2^{DD}$-3myc ($Arg^{203}$ and $Ser^{209}$ mutated to Asp), GST-MKK10-$2^{KR}$-3myc ($Lys^{81}$ mutated to Arg), or GST-3myc was combined with GST-WRKY31-3flag (each recombinant protein 2 μg) and incubated with EZview Red anti-c-Myc affinity gels (Sigma-Aldrich, E6654) with moderate shaking at 4 °C for 3 h. The beads were washed five times for 5 min with IP buffer (50 mM Tris-HCl, pH 7.4, 150 mM NaCl, 1 mM EDTA, 0.1% [v/v] Triton X-100). Proteins bound to the affinity gels were eluted by boiling the beads in 100 μL 1× Laemmli SDS loading buffer. The immunocomplexes were separated on 10% polyacrylamide gels, blotted onto PVDF membranes, and detected using horseradish peroxidase (HRP)-conjugated anti-Flag (Sigma-Aldrich, A8592, 1: 10,000 dilution) and HRP-conjugated anti-Myc (Sungene Biotech, LK8003, 1: 10,000 dilution) antibodies.

## BiFC assay

BiFC assays were performed as described previously (Kamigaki et al. 2016; Liu et al. 2016). The coding sequences of *OsWRKY31*, *OsMPK3*, *OsMPK4*, *OsMPK6*, and *OsMKK10-2* were constructed in-frame with $YFP^N$ (N-terminal YFP) and/or $YFP^C$ (C-terminal YFP). For multicolor BiFC analysis, OsMPK3, OsWRKY31, and OsWRKY45 were fused with $CFP^N$ or $CFP^C$, whereas OsMKK10-$2^{KR}$ was fused with $YFP^N$. Each plasmid was introduced into *A. tumefaciens* EHA105, and then appropriate combinations of BiFC constructs with the nuclear localization signal-targeted dsRED (35S: dsRED-NLS) plasmid were co-infiltrated into the abaxial side of 4-wk-old *N. benthamiana* leaves with a 1 mL needleless syringe. Two days later, fluorescence was visualized with a confocal microscope (Eclipse TE2000, Nikon) using the preset settings for YFP (Ex: 514 nm, Em: 510 to 550 nm), dsRED (Ex: 557 nm, Em: 579 to 586 nm), and CFP (Ex: 458 nm, Em: 470 to 500 nm).

## Plant protein extraction and immunoblot

Total plant proteins were extracted with buffer (50 mM Tris-HCl, pH 7.5, 1 mM EDTA, 10% [v/v] glycerol, 150 mM NaCl, 1% [v/v] Triton X-100, 1 mM DTT, 1 mM PMSF, 0.1 mM MG132, 1 mM cantharidin, and 1:200 protease inhibitor cocktail) on ice for 30 min. The supernatants were collected after centrifugation at 12,000 × *g* for 10 min at 4 °C, and repeated the centrifugation again for use.

Proteins or protein–DNA complexes after separation on gels were transferred to nylon membranes. Immunoblots were performed by using appropriate dilution of each antibody and then exposed to X-ray films.

## Phosphorylation assay

Potential MPK phosphorylation (SP/TP) sites of OsWRKY31 (including S2, S6, S101, S133, and T143) were sequentially mutated to phosphonull (S or T substituted to A) mutants and cloned for protein expression. OsWRKY31 and each mutant protein were subjected to phosphorylation with GST-MPK4-3myc. Phosphorylation mixture was 4:1:2 for OsWRKY31 (2 μg), OsMKK10-2, and OsMPK recombinant protein, in 100 μL volume containing 50 mM Tris-HCl (pH 7.5), 10 mM $MgCl_2$, 10 mM $MnCl_2$, 1 mM DTT, and 2 mM ATP, and reacted at 30 °C for 2 h. The reactions were terminated by adding 5× SDS loading buffer. GST-WRKY31-3flag and its S6A and S101A single and double mutants were also examined for phosphorylation by OsMPK3 or OsMPK6 in combination with OsMKK10-2. Dephosphorylation was carried out by addition of 0.5 μL calf intestinal alkaline phosphatase (CIAP) and appropriate amount of 10× alkaline buffer provided by the supplier into aliquot phosphorylation mixture and incubated at 37 °C for 1 h. The denatured samples were separated on Phos-tag gels and analyzed by immunoblots. To detect phosphorylation of OsMPKs and OsWRKY31 in plants, anti-pTEpY (Cell Signaling Technology, 9101S, 1:2,000 dilution) and anti-W31pS6 (ChinaPeptides, 2286-R4, 1:10,000) were used in immunoblotting.

## Electrophoretic mobility shift assay

The W-box containing DNA elements were derived from the promoter region of *OsPR1b* and labeled on 3′ end with biotin. EMSA was performed in a 20 μL reaction volume (10 mM Tris-HCl, pH 7.5, 50 mM NaCl, 1 mM DTT, 1 mM EDTA, and 5% [v/v] glycerol) containing about 2 μg recombinant protein, 0.03 μM biotin-labeled probe, and designated amount of competitor probes if required, at 25 °C for 30 min. The reaction was terminated by addition of 2 μL 10× loading buffer (250 mM Tris-HCl, pH 8.0, and 40% [v/v] glycerol), separated on 6% native polyacrylamide gels, and then transferred onto PVDF membranes for immunoblot using HRP-conjugated anti-Biotin antibody (Thermo Fisher 89880).

## Ubiquitination assay

Ubiquitination assay was performed by following the method described previously with slight modification (Chen et al. 2021). Each 30 μL reaction mixture contained 50 ng recombinant wheat (*Triticum aestivum*) ubiquitin-activating enzyme E1 (GI: 136632), 100 ng human ubiquitin-binding enzyme E2 (UBCH5b), 5 μg ubiquitin protein (UBQ14, At4g02890), 500 ng GST-REIW1-3myc, and 2 μg OsWRKY31 substrate or its mutant in a reaction buffer (50 mM Tris-HCl pH 7.5, 10 mM $MgCl_2$, 2 mM DTT, and 5 mM ATP) and incubated at 30 °C for 1 h. The reaction was stopped by adding 5× SDS loading buffer. Samples were separated by 10% SDS-PAGE gel and analyzed by immunobloting with anti-Ubiquitin (Sigma-Aldrich, U0508,

1:10,000 dilution) and HRP-conjugated anti-Flag (Sigma-Aldrich, A8592, 1: 10,000 dilution) antibodies.

## Protein degradation assay

To investigate whether the stability of OsWRKY31 is related with OsREIW1, the leaves of Ubi:REIW1-3myc, *reiw1ko*, and ZH17 seedlings grown hydroponically for 1 wk were used to extract the total proteins in buffer (50 mM Tris-HCl, pH 7.5, 1 mM EDTA, 10% [v/v] glycerol, 150 mM NaCl, 1% [v/v] Triton X-100, and 1 mM DTT). The protein extracts (about 500 μg) were incubated with GST-WRKY31-3flag (2 μg) for designated time points at 25 °C. The protein samples were separated and analyzed by immunobloting with HRP-conjugated anti-Flag (Sigma-Aldrich, A8592, 1: 10,000 dilution).

## GUS and LUC assays

Whole seedlings or various tissues were collected for GUS staining in the staining buffer (50 mM sodium phosphate at pH 7.0, 0.5 mM $K_3Fe[CN]_6$, 0.5 mM $K_4Fe[CN]_6$, 10 mM EDTA, 0.1% [v/v] Triton X-100, and 0.5 mg $mL^{-1}$ X-gluc), and 70% [v/v] ethanol was used to remove chlorophyll.

For GUS and luciferin (LUC) activities, the samples were homogenized in liquid nitrogen and lysed in 200 μL GUS I buffer (50 mM sodium phosphate, pH 7.0, 10 mM EDTA, 0.1% [v/v] Triton X-100, and 10 mM β-mercaptoethanol). After centrifugation, 5 μL supernatant was incubated with 45 μL GUS II buffer (GUS I buffer/methanol/20 mM 4-methyl umbelliferone glucuronide [MUG] = 7/4/1) for 30 min at 37 °C in the darkness, and the reaction was terminated by addition of 200 μL 0.2 M $Na_2CO_3$. Fluorescent product 4-methylumbelliferone (MU) was measured at Ex: 360 nm and Em: 485 nm using Multiscan Spectrum (TECAN F200). The values were calibrated against a standard curve prepared with known concentrations of MU. For LUC activity, 5 μL supernatant was added to 100 μL LR buffer (20 mM Tricine, pH 7.8, 26.7 mM $MgSO_4$, 0.1 mM EDTA, 2 mM DTT, and 5 μM ATP). After addition of 15 μL LUC, chemiluminescence was immediately measured using TECAN F200. The protein contents were detected using BSA method.

## Transcriptional activity assay

The Wbox:GUS reporter plasmid was constructed by fusion the W-box and 35S mini-promoter to *GUS* gene. The reporter and effector plasmids were transferred separately into *A. tumefaciens* EHA105 and then co-infiltrated into leaves of *N. benthamiana* with designated combinations. When chitin treatment required, the chitin solution (200 μg $mL^{-1}$) was smeared on the injection sites 3 h before the samplings. GUS and LUC activities were determined 48 h after the agroinfiltration.

## Rt-qPCR analysis

Total RNAs of various tissues was extracted via the TRIzol method and treated with DNase I to remove possible DNA contaminations. Two micrograms of total RNAs were transcribed with random hexamers and oligo$(dT)_{18}$ primers using Moloney murine leukemia virus (M-MLV) reverse transcriptase (Takara). The relative transcript levels were quantified using SYBR Green PCR MasterMix (Takara) and normalized to the ubiquitin gene (*OsUBQ*, XM_01587471). The relative expression level of each gene was analyzed using the delta–delta Ct method. Gene-specific primers used in Reverse transcription quantitative PCR (RT-qPCR) are listed in Supplemental Table S1.

## Determination of metabolites

Compound extraction and determination were described previously (Liang et al. 2017). Briefly, the leaves or roots freeze-dried (approximate 25 mg for each replicate) were extracted with 90% [v/v] aqueous methanol containing 0.1% [v/v] formic acid and internal standards of 10 ng $D_6$ABA and 0.05 ng lidocaine. After dry of the supernatants by nitrogen gas, the residues were dissolved in 0.1 mL of 90% aqueous ethanol containing 0.1% formic acid for LC-MS/MS. Chemicals were separated by a $C_{18}$ column (2.1 × 150 mm, 3 μm, Phenomenex) on Agilent 1260 separation module (Agilent).

## Statistical analysis

GraphPad Prism 8.0 and Microsoft Office Excel were used for statistical analysis of the numerical data. Significant differences between two groups were analyzed by using the one-tailed or two-tailed Student's *t*-test. Significant differences between multiple samples were determined by one-way analysis of variance (ANOVA) followed by Duncan's multiple range test with SPSS statistics software. Statistical data are provided in Supplemental Data Set 1.

## Phylogenetic analysis

The full-length amino acid sequences of 10 *Arabidopsis* and one maize MKK proteins combine with eight rice MKK proteins were aligned by ClustalW, and the neighbor-joining tree was constructed using MEGA7.0 with 1,000 bootstrap replicates.

## Accession numbers

Sequence data from this article can be found in the GenBank data libraries or Rice Genome Annotation Project Database under accession numbers showed below and also listed in Supplemental Table S1. OsWRKY11 (LOC_Os01g43650), OsWRKY31 (LOC_Os03g20550), OsWRKY45 (LOC_Os05g25770), OsWRKY76 (LOC_Os09g25060), OsMKK10-2 (LOC_Os03g12390), OsMPK3 (LOC_Os03g17700), OsMPK4 (LOC_Os10g38950), OsMPK6 (LOC_Os06g06090), OsAOS2 (LOC_Os03g12500), OsLOX2 (LOC_Os03g08220), OsAUX3 (LOC_Os05g37470), OsPIN2 (LOC_Os06g44970), OsARF12 (LOC_Os04g57610), OsARF16 (LOC_Os06g09660), OsYUCCA1 (LOC_Os01g45760), OsYUCCA4 (LOC_Os01g12490), OsGH3.1 (LOC_Os01g57610), OsGH3.2 (LOC_Os01g55940), OsGH3.3 (LOC_Os01g12160), OsGH3.4 (LOC_Os05g42150), OsGH3.5 (LOC_Os05g50890), OsGH3.6 (LOC_Os05g05180), OsGH3.7 (LOC_Os06g30440), OsGH3.8

(LOC_Os07g40290), OsGH3.9 (LOC_Os07g38890), OsGH3.10 (LOC_Os07g38860), OsGH3.11 (LOC_Os07g47490), OsGH3.12 (LOC_Os11g08340), OsGH3.13 (LOC_Os11g32520), OsKS1 (LOC_Os04g52230), OsKS4 (LOC_Os04g10060), OsPR1a (LOC_Os07g03710), OsPR1b (LOC_Os07g03600), OsPUB6 (LOC_Os06g46770), OsREIW1 (LOC_Os04g44820).

## Acknowledgments

We thank Prof. Chuanzao Mao and Prof. De An Jiang (Zhejiang University) for providing OsPIN2pro:GUS seeds and DR5-GFP plasmid, respectively. We thank Dr. Qian Chen (China Agricutural University) for help of ubiquitination and providing the plasmids, Ms. Yi Sun for assistance of rice transformation, Mr. Zongliang Chen (Yangzhou University) for help of field management. We thank Prof. Sheng Yang He (Duke University), Prof. Kabin Xie (Huazhong Agricutural University), and Prof. Jun Fan (China Agricutural University) for useful discussion and suggestions.

## Author contributions

X.C. and Z.G. conceptualized and supervised the project. S.W., S.H., and X.Z. performed most of the experiments. L.G., J.Z., F.L., and Q.H. participated in some experiments. C.Z. initiated the project. Z.G. and X.C. drafted the manuscript. All authors contributed to review and editing the manuscript.

## Supplemental data

The following materials are available in the online version of this article.

**Supplemental Figure S1**. Interaction of OsWRKY31 with OsMPKs.

**Supplemental Figure S2**. Autophosphorylation of OsMKK10-2 and activation of *OsMKK10-2* increased phosphorylation of OsMPKs.

**Supplemental Figure S3**. Identification of *mkk10-2ko*, *mpk3ko*, and *w31ko* mutants.

**Supplemental Figure S4**. Characterization of αW31pS6 antibody and induction of OsWRKY31 accumulation by chitin.

**Supplemental Figure S5**. *OsWRKY31* and *OsMKK10-2* altered rice disease resistance.

**Supplemental Figure S6**. Phylogenetic analysis of OsMKK10-2.

**Supplemental Figure S7**. Expression of *OsGH3* family genes in Dex-induced *OsMKK10-2* plants.

**Supplemental Figure S8**. *OsWRKY31* is implication in *OsMKK10-2* inhibition of seedling growth.

**Supplemental Figure S9**. Induction of *OsMKK10-2* and activation of *OsMKK10-2*-regulated gene expression in favor of defense over growth.

**Supplemental Figure S10**. Analysis of phytohormone contents.

**Supplemental Figure S11**. Induction of *OsMKK10-2* and *OsWRKY31* by chitin and knockout of *OsMKK10-2* and *OsWRKY31* compromised chitin-induced gene expression.

**Supplemental Figure S12**. Antagonistic effect of SA and MeJA to IAA on gene expression in leaves.

**Supplemental Figure S13**. Analyses of OsWRKY31 phosphorylation sites.

**Supplemental Figure S14**. Phosphomimetic OsWRKY31$^{S6DS101D}$ enhanced DNA-binding and resistance to rice blast fungus.

**Supplemental Figure S15**. OsREIW1 expression, localization, and self-ubiquitination activity.

**Supplemental Table S1**. Primers sequences used in this study.

**Supplemental Data Set 1**. Statistical data.

## Funding

This work was supported by the National Natural Science Foundation of China (U22A20463, 31972253, and 31571947), the National Key Research and Development Program of China (2016YFD0100601), and Frontiers Science Center for Molecular Design Breeding.

*Conflict of interest statement.* The authors declare no conflict of interests.

## References

**Achnine L, Blancaflor EB, Rasmussen S, Dixon RA**. Colocalization of L-phenylalanine ammonia-lyase and cinnamate 4-hydroxylase for metabolic channeling in phenylpropanoid biosynthesis. Plant Cell. 2004:**16**(11): 3098–3109. https://doi.org/10.1105/tpc.104.024406

**Andreasson E, Ellis B**. Convergence and specificity in the *Arabidopsis* MAPK nexus. Trends Plant Sci. 2010:**15**(2): 106–113. https://doi.org/10.1016/j.tplants.2009.12.001

**Cai Y, Chen X, Xie K, Xing Q, Wu Y, Li J, Du C, Sun Z, Guo Z**. Dlf1, a WRKY transcription factor, is involved in the control of flowering time and plant height in rice. PLoS One. 2014:**9**(7): e102529. https://doi.org/10.1371/journal.pone.0102529

**Chen Q, Liu R, Wu Y, Wei S, Wang Q, Zheng Y, Xia R, Shang X, Yu F, Yang X, et al.** ERAD-related E2 and E3 enzymes modulate the drought response by regulating the stability of PIP2 aquaporins. Plant Cell. 2021:**33**(8): 2883–2898. https://doi.org/10.1093/plcell/koab141

**Chen X, Li C, Wang H, Guo Z**. WRKY transcription factors: evolution, binding, and action. Phytopathol Res. 2019:**1**(1): 13. https://doi.org/10.1186/s42483-019-0022-x

**Chen Y, Fan X, Song W, Zhang Y, Xu G**. Over-expression of *OsPIN2* leads to increased tiller numbers, angle and shorter plant height through suppression of *OsLAZY1*. Plant Biotechnol J. 2012:**10**(2): 139–149. https://doi.org/10.1111/j.1467-7652.2011.00637.x

**Chen Z, Agnew JL, Cohen JD, He P, Shan L, Sheen J, Kunkel BN**. *Pseudomonas syringae* type III effector AvrRpt2 alters *Arabidopsis thaliana* auxin physiology. Proc Natl Acad Sci USA. 2007:**104**(50): 20131–20136. https://doi.org/10.1073/pnas.0704901104

**Dai Y, Wang H, Li B, Huang J, Liu X, Zhou Y, Mou Z, Li J**. Increased expression of MAP KINASE KINASE7 causes deficiency in polar auxin transport and leads to plant architectural abnormality in

*Arabidopsis*. Plant Cell. 2006:**18**(2): 308–320. https://doi.org/10.1105/tpc.105.037846

**Ding X, Cao Y, Huang L, Zhao J, Xu C, Li X, Wang S**. Activation of the indole-3-acetic acid–amido synthetase GH3-8 suppresses expansin expression and promotes salicylate-and jasmonate-independent basal immunity in rice. Plant Cell. 2008:**20**(1): 228–240. https://doi.org/10.1105/tpc.107.055657

**Domingo C, Andrés F, Tharreau D, Iglesias DJ, Talón M**. Constitutive expression of *OsGH3.1* reduces auxin content and enhances defense response and resistance to a fungal pathogen in rice. Mol Plant Microbe Interact. 2009:**22**(2): 201–210. https://doi.org/10.1094/MPMI-22-2-0201

**Gao Y, Zhang Y, Zhang D, Dai X, Estelle M, Zhao Y**. Auxin binding protein 1 (ABP1) is not required for either auxin signaling or *Arabidopsis* development. Proc Natl Acad Sci USA. 2015:**112**(7): 2275–2280. https://doi.org/10.1073/pnas.1500365112

**Guo T, Chen K, Dong N-Q, Shi C-L, Ye W-W, Gao J-P, Shan J-X, Lin H-X**. *GRAIN SIZE AND NUMBER1* negatively regulates the OsMKKK10-OsMKK4-OsMPK6 cascade to coordinate the trade-off between grain number per panicle and grain size in rice. Plant Cell. 2018:**30**(4): 871–888. https://doi.org/10.1105/tpc.17.00959

**Hamel L-P, Nicole M-C, Sritubtim S, Morency M-J, Ellis M, Ehlting J, Beaudoin N, Barbazuk B, Klessig D, Lee J**. Ancient signals: comparative genomics of plant MAPK and MAPKK gene families. Trends Plant Sci. 2006:**11**(4): 192–198. https://doi.org/10.1016/j.tplants.2006.02.007

**Hayafune M, Berisio R, Marchetti R, Silipo A, Kayama M, Desaki Y, Arima S, Squeglia F, Ruggiero A, Tokuyasu K**. Chitin-induced activation of immune signaling by the rice receptor CEBiP relies on a unique sandwich-type dimerization. Proc Natl Acad Sci USA. 2014:**111**(3): E404–E413. https://doi.org/10.1073/pnas.1312099111

**Hiei Y, Ohta S, Komari T, Kumashiro T**. Effifficient transformation of rice (*Oryza sativa* L.) mediated by *Agrobacterium* and sequence analysis of the boundaries of the T-DNA. Plant J. 1994:**6**(2): 271–282. https://doi.org/10.1046/j.1365-313X.1994.6020271.x

**Jia W, Li B, Li S, Liang Y, Wu X, Ma M, Wang J, Gao J, Cai Y, Zhang Y**. Mitogen-activated protein kinase cascade MKK7-MPK6 plays important roles in plant development and regulates shoot branching by phosphorylating PIN1 in *Arabidopsis*. PLoS Biol. 2016:**14**(9): e1002550. https://doi.org/10.1371/journal.pbio.1002550

**Jones JD, Dangl JL**. The plant immune system. Nature. 2006:**444**(7117): 323–329. https://doi.org/10.1038/nature05286

**Kamigaki A, Nito K, Hikino K, Goto-Yamada S, Nishimura M, Nakagawa T, Mano S**. Gateway vectors for simultaneous detection of multiple protein-protein interactions in plant cells using bimolecular fluorescence complementation. PLoS One. 2016:**11**(8): e0160717. https://doi.org/10.1371/journal.pone.0160717

**Kazan K**. Auxin and the integration of environmental signals into plant root development. Ann Bot. 2013:**112**(9): 1655–1665. https://doi.org/10.1093/aob/mct229

**Kidd BN, Kadoo NY, Dombrecht B, Tekeoglu M, Gardiner DM, Thatcher LF, Aitken EA, Schenk PM, Manners JM, Kazan K**. Auxin signaling and transport promote susceptibility to the root-infecting fungal pathogen *Fusarium oxysporum* in *Arabidopsis*. Mol Plant Microbe Interact. 2011:**24**(6): 733–748. https://doi.org/10.1094/MPMI-08-10-0194

**Kishi-Kaboshi M, Okada K, Kurimoto L, Murakami S, Umezawa T, Shibuya N, Yamane H, Miyao A, Takatsuji H, Takahashi A**. A rice fungal MAMP-responsive MAPK cascade regulates metabolic flow to antimicrobial metabolite synthesis. Plant J. 2010:**63**(4): 599–612. https://doi.org/10.1111/j.1365-313X.2010.04264.x

**Li X, Yang D-L, Sun L, Li Q, Mao B, He Z**. The systemic acquired resistance regulator *OsNPR1* attenuates growth by repressing auxin signaling through promoting IAA-amido synthase expression. Plant Physiol. 2016:**172**(1): 546–558. https://doi.org/10.1104/pp.16.00129

**Liang X, Chen X, Li C, Fan J, Guo Z**. Metabolic and transcriptional alternations for defense by interfering *OsWRKY62* and *OsWRKY76* transcriptions in rice. Sci Rep. 2017:**7**(1): 2474. https://doi.org/10.1038/s41598-017-02643-x

**Liu H, Liu B, Lou S, Bi H, Tang H, Tong S, Song Y, Chen N, Zhang H, Jiang Y, et al.** CHYR1 Ubiquitinates the phosphorylated WRKY70 for degradation to balance immunity in *Arabidopsis thaliana*. New Phytol. 2021:**230**(3): 1095–1109. https://doi.org/10.1111/nph.17231

**Liu J, Chen X, Liang X, Zhou X, Yang F, Liu J, He SY, Guo Z**. Alternative splicing of rice *WRKY62* and *WRKY76* transcription factor genes in pathogen defense. Plant Physiol. 2016:**171**(2): 1427–1442. https://doi.org/10.1104/pp.15.01921

**Ma H, Chen J, Zhang Z, Ma L, Yang Z, Zhang Q, Li X, Xiao J, Wang S**. MAPK Kinase 10.2 promotes disease resistance and drought tolerance by activating different MAPKs in rice. Plant J. 2017:**92**(4): 557–570. https://doi.org/10.1111/tpj.13674

**Ma H, Li J, Ma L, Wang P, Xue Y, Yin P, Xiao J, Wang S**. Pathogen-inducible OsMPKK10.2–OsMPK6 cascade phosphorylates the Raf-like kinase OsEDR1 and inhibits its scaffold function to promote rice disease resistance. Mol Plant. 2021:**14**(4): 620–632. https://doi.org/10.1016/j.molp.2021.01.008

**Ma Z, Zhu P, Shi H, Guo L, Zhang Q, Chen Y, Chen S, Zhang Z, Peng J, Chen J**. PTC-bearing mRNA elicits a genetic compensation response via Upf3a and COMPASS components. Nature. 2019:**568**(7751): 259–263. https://doi.org/10.1038/s41586-019-1057-y

**Miao Y, Laun TM, Smykowski A, Zentgraf U**. *Arabidopsis* MEKK1 can take a short cut: it can directly interact with senescence-related WRKY53 transcription factor on the protein level and can bind to its promoter. Plant Mol Biol. 2007:**65**(1-2): 63–76. https://doi.org/10.1007/s11103-007-9198-z

**Min HJ, Cui LH, Oh TR, Kim JH, Kim TW, Kim WT**. OsBZR1 turnover mediated by OsSK22-regulated U-box E3 ligase OsPUB24 in rice BR response. Plant J. 2019:**99**(3): 426–438. https://doi.org/10.1111/tpj.14332

**Navarro L, Dunoyer P, Jay F, Arnold B, Dharmasiri N, Estelle M, Voinnet O, Jones JD**. A plant miRNA contributes to antibacterial resistance by repressing auxin signaling. Science. 2006:**312**(5772): 436–439. https://doi.org/10.1126/science.1126088

**Pollmann S, Springer A, Rustgi S, von Wettstein D, Kang C, Reinbothe C, Reinbothe S**. Substrate channeling in oxylipin biosynthesis through a protein complex in the plastid envelope of *Arabidopsis thaliana*. J Exp Bot. 2019:**70**(5): 1483–1495. https://doi.org/10.1093/jxb/erz015

**Qi Y, Wang S, Shen C, Zhang S, Chen Y, Xu Y, Liu Y, Wu Y, Jiang D**. OsARF12, a transcription activator on auxin response gene, regulates root elongation and affects iron accumulation in rice (*Oryza sativa*). New Phytol. 2012:**193**(1): 109–120. https://doi.org/10.1111/j.1469-8137.2011.03910.x

**Reyna NS, Yang Y**. Molecular analysis of the rice MAP kinase gene family in relation to *Magnaporthe grisea* infection. Mol Plant Microbe Interact. 2006:**19**(5): 530–540. https://doi.org/10.1094/MPMI-19-0530

Rice WRKY Working Group. Nomenclature report on rice WRKY's-Conflict regarding gene names and its solution. Rice. 2012:**5**(1): 3. https://doi.org/10.1186/1939-8433-5-3

**Rossi A, Kontarakis Z, Gerri C, Nolte H, Hölper S, Krüger M, Stainier DY**. Genetic compensation induced by deleterious mutations but not gene knockdowns. Nature. 2015:**524**(7564): 230–233. https://doi.org/10.1038/nature14580

**Sato Y, Takehisa H, Kamatsuki K, Minami H, Namiki N, Ikawa H, Ohyanagi H, Sugimoto K, Antonio BA, Nagamura Y**. RiceXPro Version 3.0: expanding the informatics resource for rice transcriptome. Nucleic Acids Res. 2013:**41**(D1): D1206–D1213. https://doi.org/10.1093/nar/gks1125

**Shan D, Wang C, Zheng X, Hu Z, Zhu Y, Zhao Y, Jiang A, Zhang H, Shi K, Bai Y, et al.** MKK4-MPK3-WRKY17-mediated salicylic acid degradation increases susceptibility to Glomerella leaf spot in apple. Plant Physiol. 2021:**186**(2): 1202–1219. https://doi.org/10.1093/plphys/kiab108

**Shen C, Yue R, Sun T, Zhang L, Yang Y, Wang H**. OsARF16, a transcription factor regulating auxin redistribution, is required for iron deficiency response in rice (*Oryza sativa* L.). Plant Sci. 2015:**231**: 148–158. https://doi.org/10.1016/j.plantsci.2014.12.003

**Shen X, Yuan B, Liu H, Li X, Xu C, Wang S**. Opposite functions of a rice mitogen-activated protein kinase during the process of resistance against *Xanthomonas oryzae*. Plant J. 2010:**64**(1): 86–99. https://doi.org/10.1111/j.1365-313X.2010.04306.x

**Shimono M, Sugano S, Nakayama A, Jiang CJ, Ono K, Toki S, Takatsuji H**. Rice WRKY45 plays a crucial role in benzothiadiazole-inducible blast resistance. Plant Cell. 2007:**19**(6): 2064–2076. https://doi.org/10.1105/tpc.106.046250

**Singh P, Sinha AK**. A positive feedback loop governed by SUB1A1 interaction with MITOGEN-ACTIVATED PROTEIN KINASE3 imparts submergence tolerance in rice. Plant Cell. 2016:**28**(5): 1127–1143. https://doi.org/10.1105/tpc.15.01001

**Tian X, Li X, Zhou W, Ren Y, Wang Z, Liu Z, Tang J, Tong H, Fang J, Bu Q**. Transcription factor OsWRKY53 positively regulates brassinosteroid signaling and plant architecture. Plant Physiol. 2017:**175**(3): 1337–1349. https://doi.org/10.1104/pp.17.00946

**Ueno Y, Yoshida R, Kishi-Kaboshi M, Matsushita A, Jiang C-J, Goto S, Takahashi A, Hirochika H, Takatsuji H**. MAP Kinases phosphorylate rice WRKY45. Plant Signal Behav. 2013:**8**(6): e24510. https://doi.org/10.4161/psb.24510

**Ueno Y, Yoshida R, Kishi-Kaboshi M, Matsushita A, Jiang C-J, Goto S, Takahashi A, Hirochika H, Takatsuji H**. Abiotic stresses antagonize the rice defence pathway through the tyrosine-dephosphorylation of OsMPK6. PLoS Pathog. 2015:**11**(10): e1005231. https://doi.org/10.1371/journal.ppat.1005231

**Wang C, Wang G, Zhang C, Zhu P, Dai H, Yu N, He Z, Xu L, Wang E**. OsCERK1-mediated chitin perception and immune signaling requires RECEPTOR-LIKE CYTOPLASMIC KINASE 185 to activate an MAPK cascade in rice. Mol Plant. 2017:**10**(4): 619–633. https://doi.org/10.1016/j.molp.2017.01.006

**Wang H, Hao J, Chen X, Hao Z, Wang X, Lou Y, Peng Y, Guo Z**. Overexpression of rice *WRKY89* enhances ultraviolet B tolerance and disease resistance in rice plants. Plant Mol Biol. 2007:**65**(6): 799–815. https://doi.org/10.1007/s11103-007-9244-x

**Wang J, Zhang X, Greene GH, Xu G, Dong X**. PABP/purine-rich motif as an initiation module for cap-independent translation in pattern-triggered immunity. Cell. 2022:**185**(17): 3186–3200.e17. https://doi.org/10.1016/j.cell.2022.06.037

**Wang L, Guo M, Li Y, Ruan W, Mo X, Wu Z, Sturrock CJ, Yu H, Lu C, Peng J, et al.** *LARGE ROOT ANGLE1*, encoding OsPIN2, is involved in root system architecture in rice. J Exp Bot. 2018:**69**(3): 385–397. https://doi.org/10.1093/jxb/erx427

**Wu KL, Guo ZJ, Wang HH, Li J**. The WRKY family of transcription factors in rice and *Arabidopsis* and their origins. DNA Res. 2005:**12**(1): 9–26. https://doi.org/10.1093/dnares/12.1.9

**Xiong L, Yang Y**. Disease resistance and abiotic stress tolerance in rice are inversely modulated by an abscisic acid-inducible mitogen-activated protein kinase. Plant Cell. 2003:**15**(3): 745–759. https://doi.org/10.1105/tpc.008714

**Xu R, Duan P, Yu H, Zhou Z, Zhang B, Wang R, Li J, Zhang G, Zhuang S, Lyu J**. Control of grain size and weight by the OsMKKK10-OsMKK4-OsMAPK6 signaling pathway in rice. Mol Plant. 2018:**11**(6): 860–873. https://doi.org/10.1016/j.molp.2018.04.004

**Yamada K, Yamaguchi K, Yoshimura S, Terauchi A, Kawasaki T**. Conservation of chitin-induced MAPK signaling pathways in rice and *Arabidopsis*. Plant Cell Physiol. 2017:**58**(6): 993–1002. https://doi.org/10.1093/pcp/pcx042

**Yamaguchi K, Yamada K, Ishikawa K, Yoshimura S, Hayashi N, Uchihashi K, Ishihama N, Kishi-Kaboshi M, Takahashi A, Tsuge S**. A receptor-like cytoplasmic kinase targeted by a plant pathogen effector is directly phosphorylated by the chitin receptor and mediates rice immunity. Cell Host Microbe. 2013:**13**(3): 347–357. https://doi.org/10.1016/j.chom.2013.02.007

**Yamamoto Y, Kamiya N, Morinaka Y, Matsuoka M, Sazuka T**. Auxin biosynthesis by the *YUCCA* genes in rice. Plant Physiol. 2007:**143**(3): 1362–1371. https://doi.org/10.1104/pp.106.091561

**Yang Y, Qi M, Mei C**. Endogenous salicylic acid protects rice plants from oxidative damage caused by aging as well as biotic and abiotic stress. Plant J. 2004:**40**(6): 909–919. https://doi.org/10.1111/j.1365-313X.2004.02267.x

**Yang Z, Ma H, Hong H, Yao W, Xie W, Xiao J, Li X, Wang S**. Transcriptome-based analysis of mitogen-activated protein kinase cascades in the rice response to *Xanthomonas oryzae* infection. Rice. 2015:**8**(1): 4. https://doi.org/10.1186/s12284-014-0038-x

**Yuan Y, Zhong S, Li Q, Zhu Z, Lou Y, Wang L, Wang J, Wang M, Li Q, Yang D**. Functional analysis of rice *NPR1*-like genes reveals that *OsNPR1/NH1* is the rice orthologue conferring disease resistance with enhanced herbivore susceptibility. Plant Biotechnol J. 2007: **5**(2): 313–324. https://doi.org/10.1111/j.1467-7652.2007.00243.x

**Zhang J, Peng Y, Guo Z**. Constitutive expression of pathogen-inducible *OsWRKY31* enhances disease resistance and affects root growth and auxin response in transgenic rice plants. Cell Res. 2008:**18**(4): 508–521. https://doi.org/10.1038/cr.2007.104

**Zhang X, Dai Y, Xiong Y, DeFraia C, Li J, Dong X, Mou Z**. Overexpression of *Arabidopsis MAP kinase kinase 7* leads to activation of plant basal and systemic acquired resistance. Plant J. 2007: **52**(6): 1066–1079. https://doi.org/10.1111/j.1365-313X.2007.03294.x

**Zhang Z, Li J, Li F, Liu H, Yang W, Chong K, Xu Y**. OsMAPK3 phosphorylates OsbHLH002/OsICE1 and inhibits its ubiquitination to activate OsTPP1 and enhances rice chilling tolerance. Dev Cell. 2017:**43**(6): 731–743.e5. https://doi.org/10.1016/j.devcel.2017.11.016

**Zhou X, Zhao C, Guo Z**. Rice MAP kinase kinase MKK10-2 triggers cell death and $H_2O_2$ production in *Nicotiana benthamiana*. Acta Phytopathol Sin. 2017:**47**(6): 767–775. https://doi.org/10.13926/j.cnki.apps.000035